GS400.02

Introduction to Photogrammetry

T. Schenk
schenk.2@osu.edu

Autumn Quarter 2005

Department of Civil and Environmental Engineering and Geodetic Science
The Ohio State University
2070 Neil Ave., Columbus, OH 43210

Contents

Chapter 1

Introduction

1.1 Preliminary Remarks

This course provides a general overview of photogrammetry, its theory and general working principles with an emphasis on concepts rather than detailed operational knowledge.

Photogrammetry is an engineering discipline and as such heavily influenced by developments in computer science and electronics. The ever increasing use of computers has had and will continue to have a great impact on photogrammetry. The discipline is, as many others, in a constant state of change. This becomes especially evident in the shift from analog to analytical and digital methods.

There has always been what we may call a technological gap between the latest findings in research on one hand and the implementation of these results in manufactured products; and secondly between the manufactured product and its general use in an industrial process. In that sense, photogrammetric practice is an industrial process. A number of organizations are involved in this process. Inventions are likely to be associated with research organizations, such as universities, research institutes and the research departments of industry. The development of a product based on such research results is a second phase and is carried out, for example, by companies manufacturing photogrammetric equipment. Between research and development there are many similarities, the major difference being the fact that the results of research activities are not known beforehand; development goals on the other hand, are accurately defined in terms of product specifications, time and cost.

The third partner in the chain is the photogrammetrist: he daily uses the instruments and methods and gives valuable feedback to researchers and developers. Fig. 1.1 illustrates the relationship among the different organizations and the time elapsed from the moment of an invention until it becomes operational and available to the photogrammetric practice.

Analytical plotters may serve as an example for the time gap discussed above. Invented in the late fifties, they were only manufactured in quantities nearly twenty years later; they are in wide spread use since the early eighties. Another example

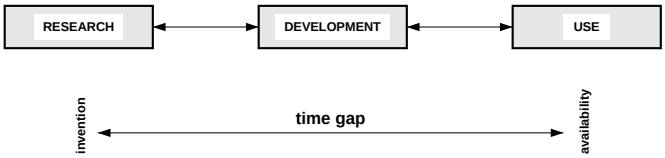

Figure 1.1: Time gap between research, development and operational use of a new method or instrument.

is aerial triangulation. The mathematical foundation was laid in the fifties, the first programs became available in the late sixties, but it took another decade before they were widely used in the photogrammetric practice.

There are only a few manufacturers of photogrammetric equipment. The two leading companies are Leica (a recent merger of the former Swiss companies Wild and Kern), and Carl Zeiss of Germany (before unification there were two separate companies: Zeiss Oberkochen and Zeiss Jena).

Photogrammetry and remote sensing are two related fields. This is also manifest in national and international organizations. The International Society of Photogrammetry and Remote Sensing (ISPRS) is a non-governmental organization devoted to the advancement of photogrammetry and remote sensing and their applications. It was founded in 1910. Members are national societies representing professionals and specialists of photogrammetry and remote sensing of a country. Such a national organization is the American Society of Photogrammetry and Remote Sensing (ASPRS).

The principle difference between photogrammetry and remote sensing is in the application; while photogrammetrists produce maps and precise three-dimensional positions of points, remote sensing specialists analyze and interpret images for deriving information about the earth's land and water areas. As depicted in Fig. 1.2 both disciplines are also related to Geographic Information Systems (GIS) in that they provide GIS with essential information. Quite often, the core of topographic information is produced by photogrammetrists in form of a digital map.

ISPRS adopted the metric system and we will be using it in this course. Where appropriate, we will occasionally use feet, particularly in regards to focal lengths of cameras. Despite considerable effort there is, unfortunately, not a unified nomenclature. We follow as closely as possible the terms and definitions laid out in (1). Students who are interested in a more thorough treatment about photogrammetry are referred to (2), (3), (4), (5). Finally, some of the leading journals are mentioned. The official journal published by ISPRS is called *Photogrammetry and Remote Sensing*. ASPRS' journal, *Photogrammetric Engineering and Remote Sensing, PERS*, appears monthly, while *Photogrammetric Record*, published by the British Society of Photogrammetry and Remote Sensing, appears six times a year. Another renowned journal is *Zeitschrift für*

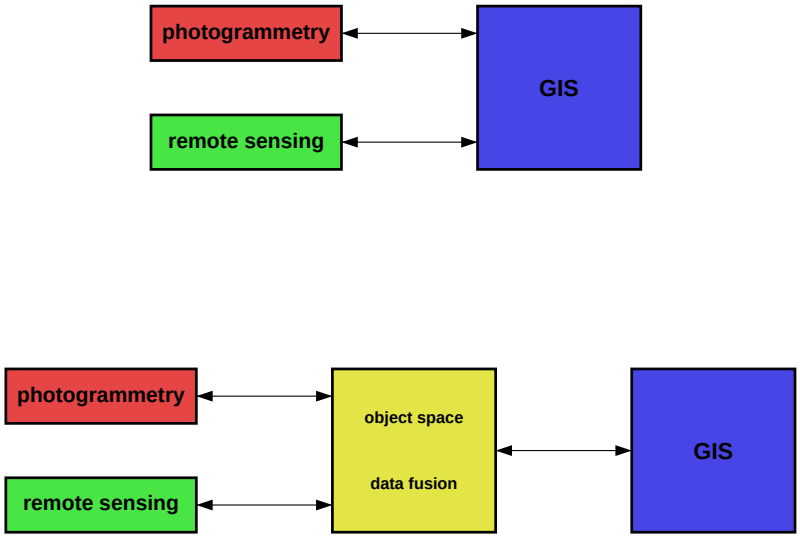

Figure 1.2: Relationship of photogrammetry, remote sensing and GIS.

Photogrammetrie und Fernerkundung, ZPF, published monthly by the German Society.

1.2 Definitions, Processes and Products

There is no universally accepted definition of photogrammetry. The definition given below captures the most important notion of photogrammetry.

> Photogrammetry is the science of obtaining reliable information about the properties of surfaces and objects without physical contact with the objects, and of measuring and interpreting this information.

The name "photogrammetry" is derived from the three Greek words *phos* or *phot* which means light, *gramma* which means letter or something drawn, and *metrein*, the noun of measure.

In order to simplify understanding an abstract definition and to get a quick grasp at the complex field of photogrammetry, we adopt a systems approach. Fig. 1.3 illustrates the idea. In the first place, photogrammetry is considered a black box. The input is characterized by obtaining reliable information through processes of recording patterns of electromagnetic radiant energy, predominantly in the form of photographic images. The output, on the other hand, comprises photogrammetric products generated within the black box whose functioning we will unravel during this course.

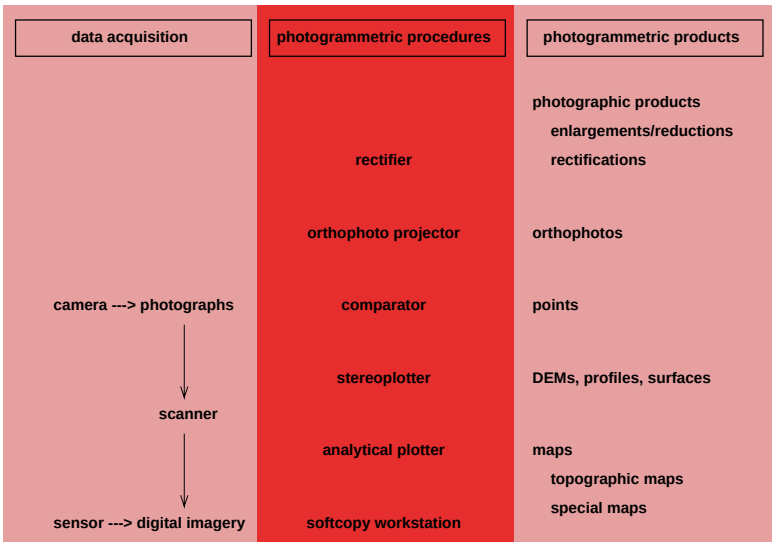

Figure 1.3: Photogrammetry portrayed as systems approach. The input is usually referred to as data acquisition, the “black box" involves photogrammetric procedures and instruments; the output comprises photogrammetric products.

1.2.1 Data Acquisition

Data acquisition in photogrammetry is concerned with obtaining reliable information about the properties of surfaces and objects. This is accomplished without physical contact with the objects which is, in essence, the most obvious difference to surveying. The remotely received information can be grouped into four categories

geometric information involves the spatial position and the shape of objects. It is the most important information source in photogrammetry.

physical information refers to properties of electromagnetic radiation, e.g., radiant energy, wavelength, and polarization.

semantic information is related to the meaning of an image. It is usually obtained by interpreting the recorded data.

temporal information is related to the change of an object in time, usually obtained by comparing several images which were recorded at different times.

As indicated in Table 1.1 the remotely sensed objects may range from planets to portions of the earth’s surface, to industrial parts, historical buildings or human bodies. The generic name for data acquisition devices is *sensor*, consisting of an optical and detector system. The sensor is mounted on a *platform*. The most typical sensors are cameras where photographic material serves as detectors. They are mounted on

Table 1.1: Different areas of specialization of photogrammetry, their objects and sensor platforms.

object	*sensor platform*	*specialization*
planet	space vehicle	space photogrammetry
earth's surface	**airplane** **space vehicle**	**aerial photogrammetry**
industrial part	tripod	industrial photogrammetry
historical building	tripod	architectural photogrammetry
human body	tripod	biostereometrics

airplanes as the most common platforms. Table 1.1 summarizes the different objects and platforms and associates them to different applications of photogrammetry.

1.2.2 Photogrammetric Products

The photogrammetric products fall into three categories: photographic products, computational results, and maps.

Photographic Products

Photographic products are derivatives of single photographs or composites of overlapping photographs. Fig. 1.4 depicts the typical case of photographs taken by an aerial camera. During the time of exposure, a latent image is formed which is developed to a negative. At the same time diapositives and paper prints are produced. Enlargements may be quite useful for preliminary design or planning studies. A better approximation to a map are rectifications. A plane rectification involves just tipping and tilting the diapositive so that it will be parallel to the ground. If the ground has a relief, then the rectified photograph still has errors. Only a differentially rectified photograph, better known as *orthophoto*, is geometrically identical with a map.

Composites are frequently used as a first base for general planning studies. Photomosaics are best known, but composites with orthophotos, called *orthophoto maps* are also used, especially now with the possibility to generate them with methods of digital photogrammetry.

Computational Results

Aerial triangulation is a very successful application of photogrammetry. It delivers 3-D positions of points, measured on photographs, in a ground control coordinate system, e.g., state plane coordinate system.

Profiles and cross sections are typical products for highway design where earthwork quantities are computed. Inventory calculations of coal piles or mineral deposits are

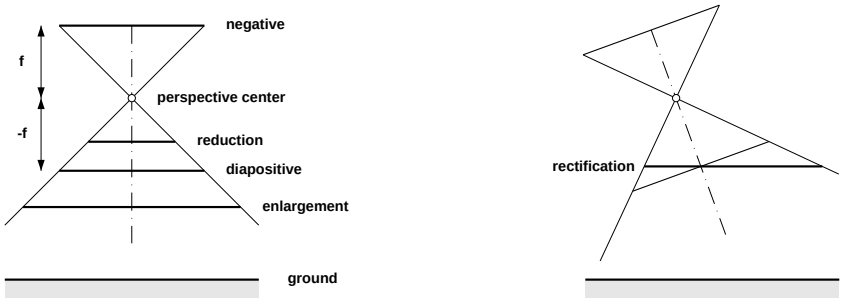

Figure 1.4: Negative, diapositive, enlargement reduction and plane rectification.

other examples which may require profile and cross section data. The most popular form for representing portions of the earth's surface is the DEM (Digital Elevation Model). Here, elevations are measured at regularly spaced grid points.

Maps

Maps are the most prominent product of photogrammetry. They are produced at various scales and degrees of accuracies. Planimetric maps contain only the horizontal position of ground features while topographic maps include elevation data, usually in the form of contour lines and spot elevations. Thematic maps emphasize one particular feature, e.g., transportation network.

1.2.3 Photogrammetric Procedures and Instruments

In our attempt to gain a general understanding of photogrammetry, we adopted a systems approach. So far we have addressed the input and output. Obviously, the task of photogrammetric procedures is to convert the input to the desired output. Let us take an aerial photograph as a typical input and a map as a typical output. Now, what are the main differences between the two? Table 1.2 lists three differences. First, the projection system is different and one of the major tasks in photogrammetry is to establish the corresponding transformations. This is accomplished by mechanical/optical means in analog photogrammetry, or by computer programs in analytical photogrammetry.

Another obvious difference is the amount of data. To appreciate this comment, let us digress for a moment and find out how much data an aerial photograph contains. We can approach this problem by continuously dividing the photograph in four parts. After a while, the ever smaller quadrants reach a size where the information they contain is not different. Such a small area is called a *pixel* when the image is stored on a computer. A pixel then is the smallest unit of an image and its value is the gray shade of that particular image location. Usually, the continuous range of gray values is divided into 256 discrete values, because 1 byte is sufficient to store a pixel. Experience tells us that the smallest pixel size is about $5\ \mu m$. Considering the size of a photograph (9 inches or 22.8 cm) we have approximately half a gigabyte (0.5 GB) of data for one

Table 1.2: Differences between photographs and maps.

	photograph	*map*	*task*
projection	central	orthogonal	transformations
data	≈ 0.5 GB	few KB	feature identification
information	explicit	implicit	and feature extraction

photograph. A map depicting the same scene will only have a few thousand bytes of data. Consequently, another important task is data reduction.

The information we want to represent on a map is explicit. By that we mean that all data is labeled. A point or a line has an attribute associated which says something about the type and meaning of the point or line. This is not the case for an image; a pixel has no attribute associate with it which would tell us what feature it belongs to. Thus, the relevant information is only implicitly available. Making information explicit amounts to identifying and extracting those features which must be represented on the map.

Finally, we refer back to Fig. 1.3 and point out the various instruments that are used to perform the tasks described above. A *rectifier* is kind of a copy machine for making plane rectifications. In order to generate orthophotos, an *orthophoto projector* is required. A *comparator* is a precise measuring instrument which lets you measure points on a diapositive (photo coordinates). It is mainly used in aerial triangulation. In order to measure 3-D positions of points in a stereo model, a *stereo plotting instrument* or *stereo plotter* for short, is used. It performs the transformation central projection to orthogonal projection in an analog fashion. This is the reason why these instruments are sometimes less officially called *analog plotters*. An *analytical plotter* establishes the transformation computationally. Both types of plotters are mainly used to produce maps, DEMs and profiles.

A recent addition to photogrammetric instruments is the *softcopy workstation*. It is the first tangible product of digital photogrammetry. Consequently, it deals with digital imagery rather than photographs.

1.3 Historical Background

The development of photogrammetry clearly depends on the general development of science and technology. It is interesting to note that the four major phases of photogrammetry are directly related to the technological inventions of photography, airplanes, computers and electronics.

Fig. 1.5 depicts the four generations of photogrammetry. Photogrammetry had its beginning with the invention of photography by Daguerre and Niepce in 1839. The first generation, from the middle to the end of last century, was very much a pioneering and experimental phase with remarkable achievements in terrestrial and balloon

photogrammetry.

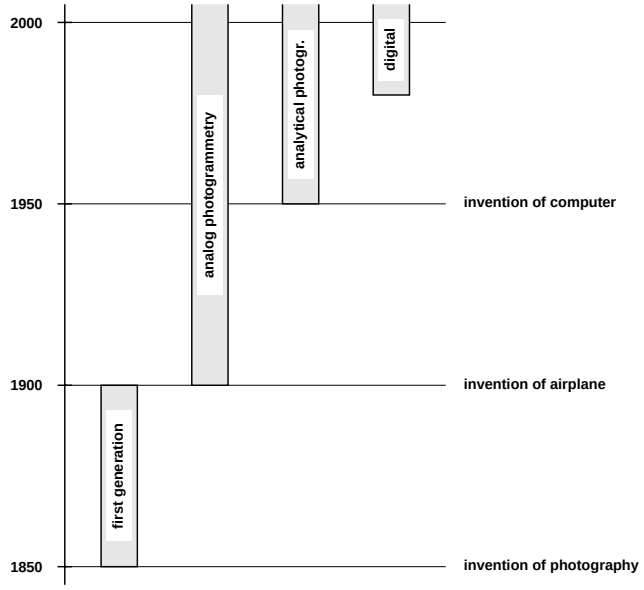

Figure 1.5: Major photogrammetric phases as a result of technological innovations.

The second generation, usually referred to as *analog photogrammetry*, is characterized by the invention of stereophotogrammetry by Pulfrich (1901). This paved the way for the construction of the first stereoplotter by Orel, in 1908. Airplanes and cameras became operational during the first world war. Between the two world wars, the main foundations of aerial survey techniques were built and they stand until today. Analog rectification and stereoplotting instruments, based on mechanical and optical technology, became widely available. Photogrammetry established itself as an efficient surveying and mapping method. The basic mathematical theory was known, but the amount of computation was prohibitive for numerical solutions and consequently all the efforts were aimed toward analog methods. Von Gruber is said to have called photogrammetry the art of avoiding computations.

With the advent of the computer, the third generation has begun, under the motto of *analytical photogrammetry*. Schmid was one of the first photogrammetrists who had access to a computer. He developed the basis of analytical photogrammetry in the fifties, using matrix algebra. For the first time a serious attempt was made to employ adjustment theory to photogrammetric measurements. It still took several years before the first operational computer programs became available. Brown developed the first block adjustment program based on bundles in the late sixties, shortly before Ackermann reported on a program with independent models as the underlying concept. As a result,

the accuracy performance of aerial triangulation improved by a factor of ten.

Apart from aerial triangulation, the analytical plotter is another major invention of the third generation. Again, we observe a time lag between invention and introduction to the photogrammetric practice. Helava invented the analytical plotter in the late fifties. However, the first instruments became only available in the seventies on a broad base.

The fourth generation, *digital photogrammetry*, is rapidly emerging as a new discipline in photogrammetry. In contrast to all other phases, digital images are used instead of aerial photographs. With the availability of storage devices which permit rapid access to digital imagery, and special microprocessor chips, digital photogrammetry began in earnest only a few years ago. The field is still in its infancy and has not yet made its way into the photogrammetric practice.

References

[1] *Multilingual Dictionary of Remote Sensing and Photogrammetry*, ASPRS, 1983, p. 343.

[2] *Manual of Photogrammetry*, ASPRS, 4th Ed., 1980, p. 1056.

[3] Moffit, F.H. and E. Mikhail, 1980. *Photogrammetry*, 3rd Ed., Harper & Row Publishers, NY.

[4] Wolf, P., 1980. *Elements of Photogrammetry*, McGraw Hill Book Co, NY.

[5] Kraus, K., 1994. *Photogrammetry*, Verd. Dümmler Verlag, Bonn.

Chapter 2

Film-based Cameras

2.1 Photogrammetric Cameras

2.1.1 Introduction

In the beginning of this chapter we introduced the term sensing device as a generic name for sensing and recording radiometric energy (see also Fig. 2.1). Fig. 2.1 shows a classification of the different types of sensing devices.

An example of an active sensing device is radar. An operational system sometimes used for photogrammetric applications is the side looking airborne radar (SLAR). Its chief advantage is the fact that radar waves penetrate clouds and haze. An antenna, attached to the belly of an aircraft directs microwave energy to the side, rectangular to the direction of flight. The incident energy on the ground is scattered and partially reflected. A portion of the reflected energy is received at the same antenna. The time elapsed between energy transmitted and received can be used to determine the distance between antenna and ground.

Passive systems fall into two categories: image forming systems and spectral data systems. We are mainly interested in image forming systems which are further subdivided into framing systems and scanning systems. In a framing system, data are acquired all at one instant, whereas a scanning system obtains the same information sequentially, for example scanline by scanline. Image forming systems record radiant energy at different portions of the spectrum. The spatial position of recorded radiation refers to a specific location on the ground. The imaging process establishes a geometric and radiometric relationship between spatial positions of object and image space.

Of all the sensing devices used to record data for photogrammetric applications, the photographic systems with metric properties are the most frequently employed. They are grouped into *aerial* cameras and *terrestrial* cameras. Aerial cameras are also called *cartographic* cameras. In this section we are only concerned with aerial cameras. *Panoramic* cameras are examples of non-metric aerial cameras. Fig. 2.2(a) depicts an aerial camera.

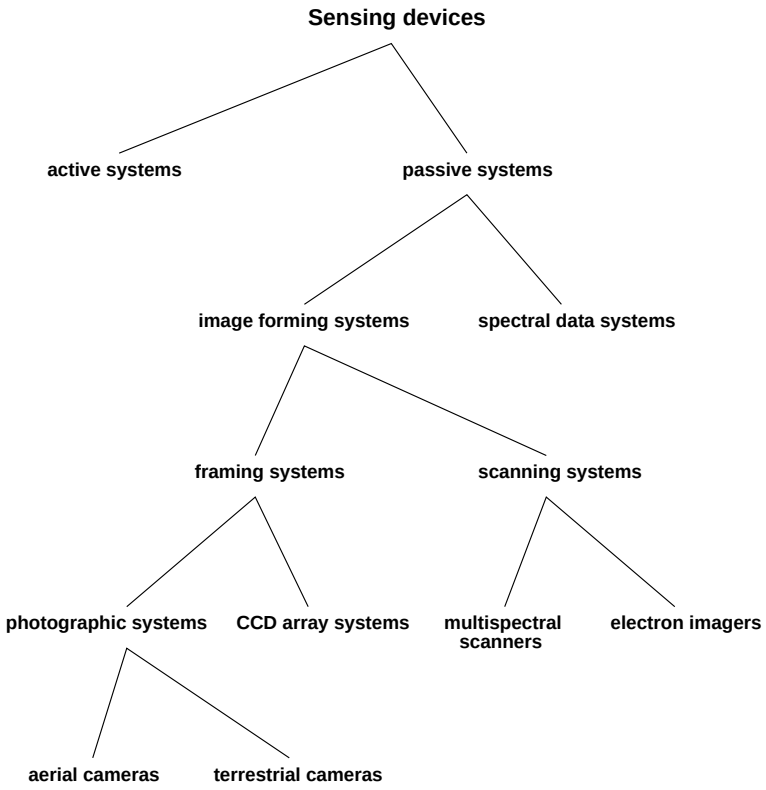

Figure 2.1: Classification of sensing devices.

2.1.2 Components of Aerial Cameras

A typical aerial camera consists of *lens assembly*, *inner cone*, *focal plane*, *outer cone*, *drive mechanism*, and *magazine*. These principal parts are shown in the schematic diagram of Fig. 2.2(b).

Lens Assembly

The lens assembly, also called *lens cone*, consists of the camera lens (objective), the diaphragm, the shutter and the filter. The diaphragm and the shutter control the exposure. The camera is focused for infinity; that is, the image is formed in the focal plane.

Fig. 2.3 shows cross sections of lens cones with different focal lengths. *Super-wide-angle* lens cones have a focal length of 88 mm (3.5 in). The other extreme are *narrow-angle* cones with a focal length of 610 mm (24 in). Between these two extremes are *wide-angle*, *intermediate-angle*, and *normal-angle* lens cones, with focal lengths of 153 mm (6 in), 213 mm (8.25 in), and 303 mm (12 in), respectively. Since the film format does not change, the *angle of coverage*, or *field* for short, changes, as well as the

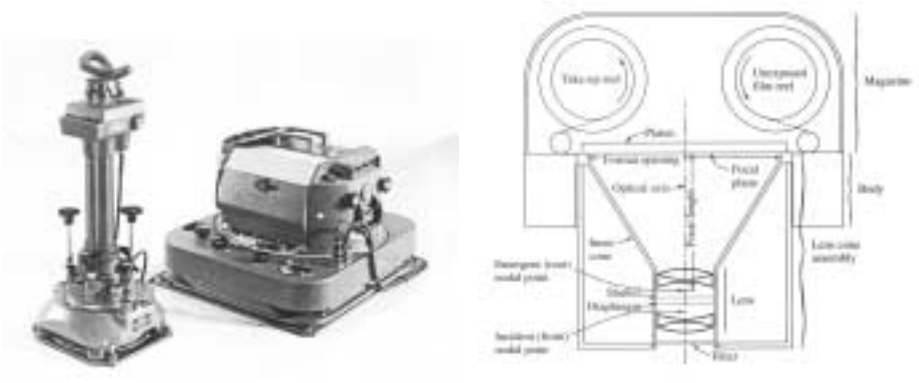

Figure 2.2: (a) Aerial camera Aviophot RC20 from Leica; (b) schematic diagram of aerial camera.

Table 2.1: Data of different lens assemblies.

	super-wide	wide-angle	inter-mediate	normal-angle	narrow-angle
focal length [mm]	88.	153.	210.	305.	610.
field [o]	119.	82.	64.	46.	24.
photo scale	7.2	4.0	2.9	2.0	1.0
ground coverage	50.4	15.5	8.3	3.9	1.0

scale. The most relevant data are compiled in Table 2.1. Refer also to Fig. 2.4 which illustrates the different configurations.

Super-wide angle lens cones are suitable for medium to small scale applications because the flying height, H, is much lower compared to a normal-angle cone (same photo scale assumed). Thus, the atmospheric effects, such as clouds and haze, are much less a problem. Normal-angle cones are preferred for large-scale applications of urban areas. Here, a super-wide angle cone would generate much more occluded areas, particularly in built-up areas with tall buildings.

Inner Cone and Focal Plane

For metric cameras it is very important to keep the lens assembly fixed with respect to the focal plane. This is accomplished by the inner cone. It consists of a metal with low coefficient of thermal expansion so that the lens and the focal plane do not change their relative position. The focal plane contains *fiducial marks*, which define the fiducial coordinate system that serves as a reference system for metric photographs. The fiducial marks are either located at the corners or in the middle of the four sides.

Usually, additional information is printed on one of the marginal strips during the

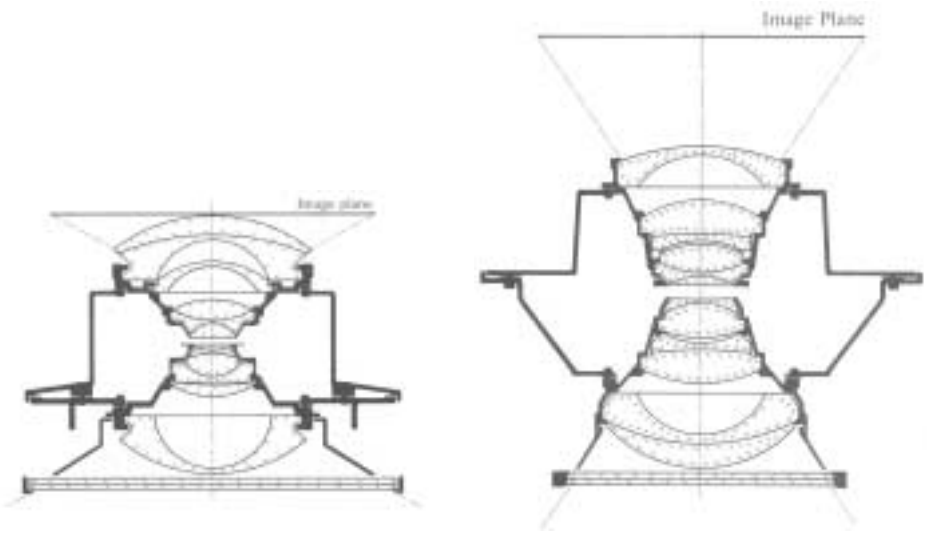

Figure 2.3: Cross-sectional views of aerial camera lenses.

time of exposure. Such information includes the date and time, altimeter data, photo number, and a level bubble.

Outer Cone and Drive Mechanism

As shown in Fig. 2.2(b) the outer cone supports the inner cone and holds the drive mechanism. The function of the drive mechanism is to wind and trip the shutter, to operate the vacuum, and to advance the film between exposures. The vacuum assures that the film is firmly pressed against the image plane where it remains flat during exposure. Non-flatness would not only decrease the image quality (blurring) but also displace points, particularly in the corners.

Magazine

Obviously, the magazine holds the film, both, exposed and unexposed. A film roll is 120 m long and provides 475 exposures. The magazine is also called film cassette. It is detachable, allowing to interchange magazines during a flight mission.

2.1.3 Image Motion

During the instance of exposure, the aircraft moves and with it the camera, including the image plane. Thus, a stationary object is imaged at different image locations, and the image appears to move. Image motion results not only from the forward movement of the aircraft but also from vibrations. Fig. 2.5 depicts the situation for forward motion.

An airplane flying with velocity v advances by a distance $D = v\,t$ during the exposure time t. Since the object on the ground is stationary, its image moves by a

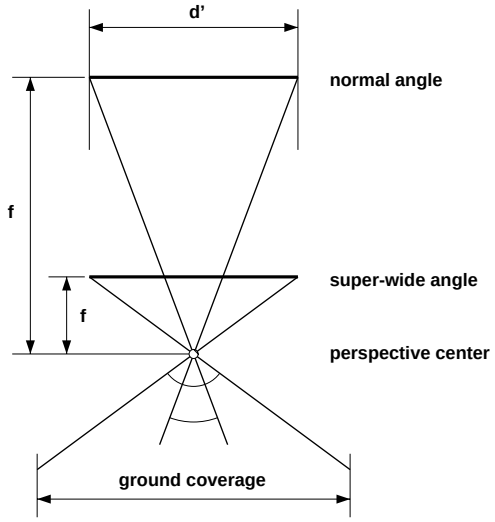

Figure 2.4: Angular coverage, photo scale and ground coverage of cameras with different focal lengths.

distance $d = D/m$ where m is the photo scale. We have

$$d = \frac{v\,t}{m} = \frac{v\,t\,f}{H} \tag{2.1}$$

with f the focal length and H the flying height.
Example:

exposure time t	1/300 sec
velocity v	300 km/h
focal length f	150 mm
flying height H	1500 m
image motion d	$28\ \mu m$

Image motion caused by vibrations in the airplane can also be computed using Eq. 2.1. For that case, vibrations are expressed as a time rate of change of the camera axis (angle/sec). Suppose the camera axis vibrates by $2^0/sec$. This corresponds to a distance $D_v = 2\,H/\rho = 52.3$ m. Since this "displacement" occurs in one second, it can be considered a velocity. In our example, this velocity is 188.4 km/sec, corresponding to an image motion of $18\,\mu m$. Note that in this case, the direction of image motion is random.

As the example demonstrates, image motion may considerably decrease the image quality. For this reason, modern aerial cameras try to eliminate image motion. There are different mechanical/optical solutions, known as *image motion compensation*. The forward image motion can be reduced by moving the film during exposure such that the

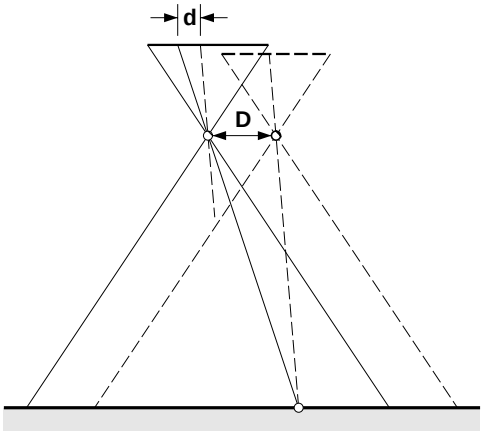

Figure 2.5: Forward image motion.

image of an object does not move with respect to the emulsion. Since the direction of image motion caused by vibration is random, it cannot be compensated by moving the film. The only measure is a shock absorbing camera mount.

2.1.4 Camera Calibration

During the process of camera calibration, the *interior orientation* of the camera is determined. The interior orientation data describe the metric characteristics of the camera needed for photogrammetric processes. The elements of interior orientation are:

1. The position of the perspective center with respect to the fiducial marks.
2. The coordinates of the fiducial marks or distances between them so that coordinates can be determined.
3. The calibrated focal length of the camera.
4. The radial and discentering distortion of the lens assembly, including the origin of radial distortion with respect to the fiducial system.
5. Image quality measures such as resolution.

There are several ways to calibrate the camera. After assembling the camera, the manufacturer performs the calibration under laboratory conditions. Cameras should be calibrated once in a while because stress, caused by temperature and pressure differences of an airborn camera, may change some of the interior orientation elements. Laboratory calibrations are also performed by specialized government agencies.

In *in-flight* calibration, a testfield with targets of known positions is photographed. The photo coordinates of the targets are then precisely measured and compared with the control points. The interior orientation is found by a least-square adjustment.

We will describe one laboratory method, known as *goniometer calibration*. This will further the understanding of the metric properties of an aerial camera.

Fig. 2.6 depicts a goniometer with a camera ready for calibration. The goniometer resembles a theodolite. In fact, the goniometer shown is a modified T4 high precision theodolite used for astronomical observations. To the far right of Fig. 2.6(a) is a collimator. If the movable telescope is aimed at the collimator, the line of sight represents the optical axis. The camera is placed into the goniometer such that its vertical axis passes through the entrance pupil. Additionally, the focal plane is aligned perpendicular to the line of sight. This is accomplished by autoreflection of the collimator. Fig. 2.6(b) depicts this situation; the fixed collimator points to the center of the grid plate which is placed in the camera's focal plane. This center is referred to as *principal point of autocollimation*, PPA.

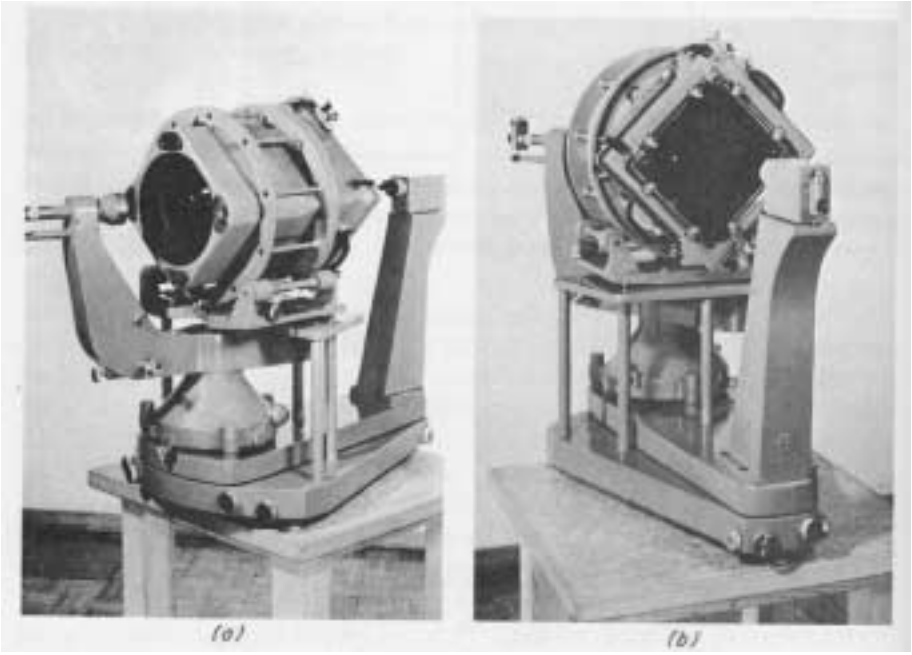

Figure 2.6: Two views of a goniometer with installed camera, ready for calibration.

Now, the measurement part of the calibration procedure begins. The telescope is aimed at the grid intersections of the grid plate, viewing through the camera. The angles subtended at the rear nodal point between the camera axis and the grid intersections are obtained by subtracting from the circle readings the zero position (reading to the collimator before the camera is installed). This is repeated for all grid intersections along the four semi diagonals.

Having determined the angles α_i permits to compute the distances d_i from the center of the grid plate (PPA) to the corresponding grid intersections i by Eq. 2.2

$$d_i = f \tan(\alpha_i) \quad (2.2)$$

$$dr_i'' = dg_i - d_i \quad (2.3)$$

The computed distances d_i are compared with the known distances dg_i of the grid plate. The differences dr_i'' result from the radial distortion of the lens assembly. Radial distortion arises from a change of lateral magnification as a function of the distance from the center.

The differences dr_i'' are plotted against the distances d_i. Fig. 2.7(a) shows the result. The curves for the four semi diagonals are quite different and it is desirable to make them as symmetrical as possible to avoid working with four sets of distortion values. This is accomplished by changing the origin from the PPA to a different point, called the *principal point of symmetry* (PPS). The effect of this change of the origin is shown in Fig. 2.7(b). The four curves are now similar enough and the average curve represents the direction-independent distortion. The distortion values for this average curve are denoted by dr_i'.

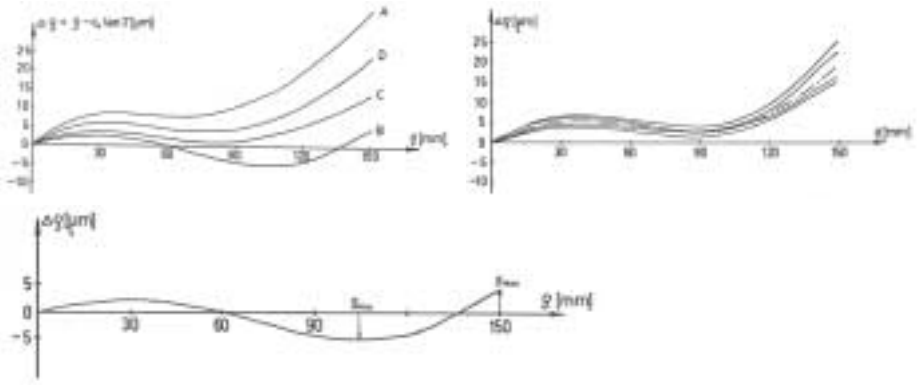

Figure 2.7: Radial distortion curves for the four semi-diagonals (a). In (b) the curves are made symmetrical by shifting the origin to PPS. The final radial distortion curve in (c) is obtained by changing the focal length from f to c.

The average curve is not yet well balanced with respect to the horizontal axis. The next step involves a rotation of the distortion curve such that $|dr_{\text{min}}| = |dr_{\text{max}}|$. A change of the focal length will rotate the average curve. The focal length with this desirable property is called *calibrated focal length, c*. Through the remainder of the text, we will be using c instead of f, that is, we use the calibrated focal length and not the optical focal length.

After completion of all measurements, the grid plate is replaced by a photosensitive plate. The telescope is rotated to the zero position and the reticule is projected through

the lens onto the plate where it marks the PPA. At the same time the fiducial marks are exposed. The processed plate is measured and the position of the PPA is determined with respect to the fiducial marks.

2.1.5 Summary of Interior Orientation

We summarize the most important elements of the interior orientation of an aerial camera by referring to Fig. 2.8. The main purpose of interior orientation is to define the position of the perspective center and the radial distortion curve. A camera with known interior orientation is called *metric* if the orientation elements do not change. An amateur camera, for example, is non-metric because the interior orientation changes every time the camera is focused. Also, it lacks a reference system for determining the PPA.

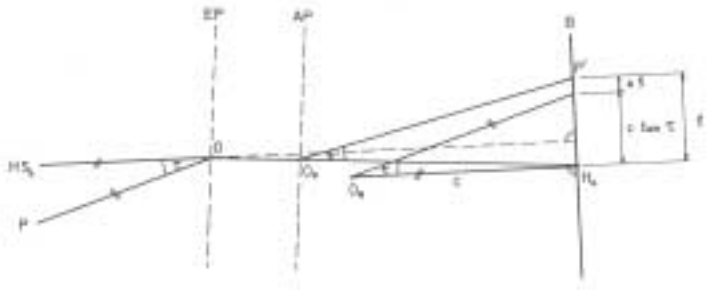

Figure 2.8: Illustration of interior orientation. EP and AP are entrance and exit pupils. they intersect the optical axis at the perspective centers O and O_p. The mathematical perspective center O_m is determined such that angles at O and O_m become as similar as possible. Point H_a, also known as principal point of autocollimation, PPA, is the vertical drop of O_m to the image plane B. The distance O_m, H_a, c, is the calibrated focal length.

1. The position of the perspective center is given by the PPA and the calibrated focal length c. The bundle rays through projection center and image points resemble most closely the bundle in object space, defined by the front nodal point and points on the ground.

2. The radial distortion curve contains the information necessary for correcting image points that are displaced by the lens due to differences in lateral magnification. The origin of the symmetrical distortion curve is at the principal point of symmetry PPS. The distortion curve is closely related to the calibrated focal length.

3. The position of the PPA and PPS is fixed with reference to the fiducial system. The intersection of opposite fiducial marks indicates the fiducial center FC. The

three centers lie within a few microns. The fiducial marks are determined by distances measured along the side and diagonally.

Modern aerial cameras are virtually distortion free. A good approximation for the interior orientation is to assume that the perspective center is at a distance c from the fiducial center.

2.2 Photographic Processes

The most widely used detector system for photogrammetric applications is based on photographic material. It is analog system with some unique properties which makes it superior to digital detectors such as CCD arrays. An aerial photograph contains on the order of one Gigabyte of data (see Chapter 1); the most advanced semiconductor chips have a resolution of $2K \times 2K$, or 4 MB of data.

In this section we provide an overview of photographic processes and properties of photographic material. The student should gain a basic understanding of exposure, sensitivity, speed and resolution of photographic emulsions.

Fig. 2.9 provides an overview of photographic processes and introduces the terms *latent image*, *negative*, *(dia)positive* and *paper print*.

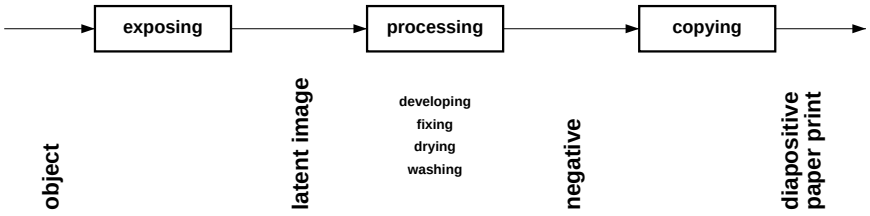

Figure 2.9: Overview of photographic processes.

2.2.1 Photographic Material

Fig. 2.10 depicts a cross-sectional view of color photography. It consists of three sensitized emulsions which are coated on the base material. To prevent transmitted light from being reflected at the base, back to the emulsion, an antihalation layer is added between emulsion and base.

The light sensitive emulsion consists of three thin layers of gelatine in which are suspended crystals of silver halide. Silver halide is inherently sensitive to near ultra violet and blue. In order for the silver halide to absorb energy at longer wavelengths, optical sensitizers, called *dyes*, are added. They have the property to transfer electromagnetic energy from yellow to near infrared to the silver halide.

A critical factor of photography is the geometrical stability of the base material. Today, most films used for photogrammetric applications (called *aerial films*), have a polyester base. It provides a stability over the entire frame of a few microns. Most of the

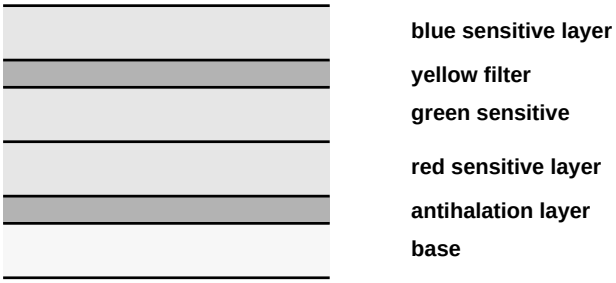

Figure 2.10: Cross section of film for color photography.

deformation occurs during the development process. It is caused by the development bath and mechanical stress to transport the film through the developer. The deformation is usually called *film shrinkage*. It consists of systematic deformations (e.g. scale factor) and random deformations (local inconsistencies, e.g. scale varies from one location to another). Most of the systematic deformations can be determined during the interior orientation and subsequently be corrected.

2.2.2 Photographic Processes

Exposure

Exposure H is defined as the quantity of radiant energy collected by the emulsion.

$$H = E\,t \tag{2.4}$$

where E is the irradiance as defined in section 2.1.4, and t the exposure time. H is determined by the exposure time and the aperture stop of the the lens system (compare vignetting diagrams in Fig. 2.16). For fast moving platforms (or objects), the exposure time should be kept short to prevent blurring. In that case, a small f-number must be chosen so that enough energy interacts with the emulsion. The disadvantage with this setting is an increased influence of aberrations.

The sensitive elements of the photographic emulsion are microscopic crystals with diameters from $0.3\ \mu m$ to $3.0\ \mu m$. One crystal is made up of 10^{10} silver halide ions. When radiant energy is incident upon the emulsion it is either reflected, refracted or absorbed. If the energy of the photons is sufficient to liberate an electron from a bound state to a mobile state then it is absorbed, resulting in a free electron which combines quickly with a silver halide ion to a silver atom.

The active product of exposure is a small aggregate of silver atoms on the surface or in the interior of the crystal. This silver speck acts as a catalyst for the development reaction where the exposed crystals are completely reduced to silver whereas the unexposed crystals remain unchanged. The exposed but undeveloped film is called *latent image*. In the most sensitive emulsions only a few photons are necessary for forming a

developable image. Therefore the amplifying factor is on the order of 10^9, one of the largest amplifications known.

Sensitivity

The sensitivity can be defined as the extent of photographic material to react to radiant energy. Since this is a function of wavelength, sensitivity is a spectral quantity. Fig. 2.11 provides an overview of emulsions with different sensitivity.

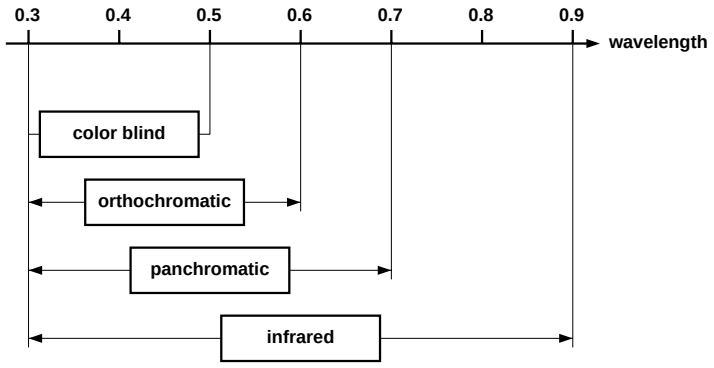

Figure 2.11: Overview of photographic material with different sensitivity range.

Silver halide emulsions are inherently only sensitive to ultra violet and blue. In order for the silver halide to absorb energy at longer wavelengths, dyes are added. The three color sensitive emulsion layers differ in the dyes that are added to silver halide. If no dyes are added the emulsion is said to be *color blind*. This may be desirable for paper prints because one can work in the dark room with red light without affecting the latent image. Of course, color blind emulsions are useless for aerial film because they would only react to blue light which is scattered most causing a diffuse image without contrast.

In *orthochromatic* emulsions the sensitivity is extended to include the green portion of the visible spectrum. *Panchromatic* emulsions are sensitive to the entire visible spectrum; *infrared* film includes the near infrared.

Colors and Filters

The visible spectrum is divided into three categories: 0.4 to 0.5 μm, 0.5 to 0.6 μm, and 0.6 to 0.7 μm. These three categories are associated to the *primary* colors of blue, green and red. All other colors, approximately 10 million, can be obtained by an additive mixture of the primary colors. For example, white is a mixture of equal portions of primary colors. If two primary colors are mixed the three *additive colors* cyan, yellow and magenta are obtained. As indicated in Table 2.2, these additive colors also result from subtracting the primary colors from white light.

Table 2.2: Primary colors and additive primary colors

.

additive color primary	*additive mixture of 2 color primaries*	*subtraction from white light*
cyan	b + g	w - r
yellow	g + r	w - b
magenta	r + b	w - g

Subtraction can be achieved by using filters. A filter with a subtractive color primary is transparent for the additive primary colors. For example, a yellow filter is transparent for green and red. Such a filter is also called *minus blue* filter. A combination of filters is only transparent for that color the filters have in common. Cyan and magenta is transparent for blue since this is their common primary color.

Filters play a very important role in obtaining aerial photography. A yellow filter, for example, prevents scattered light (blue) from interacting with the emulsion. Often, a combination of several filters is used to obtain photographs of high image quality. Since filters reduce the amount of radiant energy incident the exposure must be increased by either decreasing the f-number, or by increasing the exposure time.

Processing Color Film

Fig. 2.12 illustrates the concept of *natural color* and *false color* film material. A natural color film is sensitive to radiation of the visible spectrum. The layer that is struck first by radiation is sensitive to red, the middle layer is sensitive to green, and the third layer is sensitive to blue. During the development process the situation becomes reversed; that is, the red layer becomes transparent for red light. Wherever green was incident the red layer becomes magenta (white minus green); likewise, blue changes to yellow. If this developed film is viewed under white light, the original colors are perceived.

A closer examination of the right side of Fig. 2.12 reveals that the sensitivity of the film is shifted towards longer wavelengths. A yellow filter prevents blue light from interacting with the emulsion. The top most layer is now sensitive to near infrared, the middle layer to red and the third layer is sensitive to green. After developing the film, red corresponds to infrared, green to red, and blue to green. This explains the name false color film: vegetation reflects infrared most. Hence, forest, trees and meadows appear red.

2.2.3 Sensitometry

Sensitometry deals with the measurement of sensitivity and other characteristics of photographic material. The *density* (amount of exposure) can be measured by a *densitometer*. The density D is defined as the degree of blackening of an exposed film.

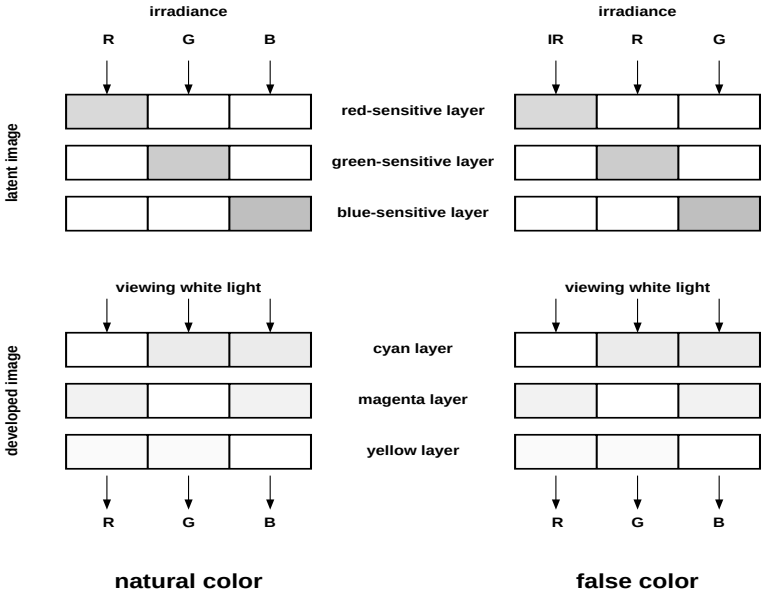

Figure 2.12: Concept of processing natural color (left) and false color film (right

.

$$D = \log(O) \tag{2.5}$$

$$O = \frac{E_i}{E_t} \tag{2.6}$$

$$T = \frac{E_t}{E_i} = \frac{1}{O} \tag{2.7}$$

$$H = E\,t \tag{2.8}$$

where

O	opacity, degree of blackening
E_i	irradiance
E_t	transmitted irradiance
T	transmittance
H	exposure

The density is a function of exposure H. It also depends on the development process. For example, the density increases with increasing development time. An underexposed latent image can be “corrected" to a certain degree by increasing the development time.

Fig. 2.13 illustrates the relationship between density and exposure. The *characteristic curve* is also called *D-log(H)* curve. Increasing exposure results in more crystals

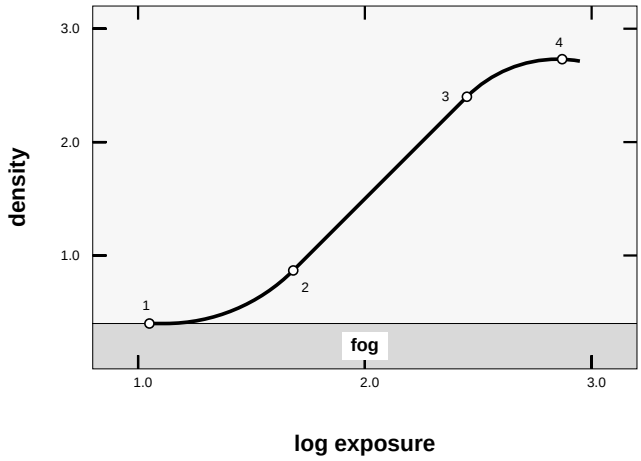

Figure 2.13: Characteristic curve of a photographic emulsion.

with silver specks that are reduced to black silver: a bright spot in the the scene appears dark in the negative.

The characteristic curve begins at a threshold value, called *fog*. An unexposed film should be totally transparent when reduced during the development process. This is not the case because the base of the film has a transmittance smaller than unity. Additionally, the transmittance of the emulsion with unexposed material is smaller than unity. Both factor contribute to fog. The lower part of the curve, between point 1 and 2, is called *toe region*. Here, the exposure is not enough to cause a readable image. The next region, corresponding to correct exposure, is characterized by a straight line (between point 2 and 3). That is, the density increases linearly with the logarithm of exposure. The slope of the straight line is called *gamma* or *contrast*. A film with a slope of 45^0 is perceived as truly presenting the contrast in the scene. A film with a higher gamma exaggerates the scene contrast. The contrast is not only dependent on the emulsion but also on the development time. If the same latent image is kept longer in the development process, its characteristic curve becomes flatter.

The straight portion of the characteristic curve ends in the *shoulder region* where the density no longer increases linearly. In fact, there is a turning point, *solarization*, where D decreases with increasing exposure (point 4 in Fig. 2.13). Clearly, this region is associated with over exposure.

2.2.4 Speed

The size and the density of the silver halide crystals suspended in the gelatine of the emulsion vary. The larger the crystal size the higher the probability that is struck by photons during the exposure time. Fewer photons are necessary to cause a latent image. Such a film would be called faster because the latent image is obtained in a shorter time period compared to an emulsion with smaller crystal size. In other words, a faster

film requires less exposure. Unfortunately, there is no universally accepted definition of speed. There is, however, a standard for determining the speed of aerial films, known as Aerial film Speed (AFS).

The exposure used to determine AFS is the point on the characteristic curve at which the density is 0.3 units above fog (see Fig. 2.14). The exposure H needed to produce this density is used in the following definition

$$\text{AFS} = \frac{3}{2\,H} \tag{2.9}$$

Note that aerial film speed differs from speed as defined by ASA. Here, the the exposure is specified which is necessary to produce a density 0.1 units above fog. Fig. 2.14 shows two emulsions with different speed and different gamma. Since emulsion A requires less exposure to produce the required density at 0.3 above fog, it is faster than emulsion B ($H_A < H_B$).

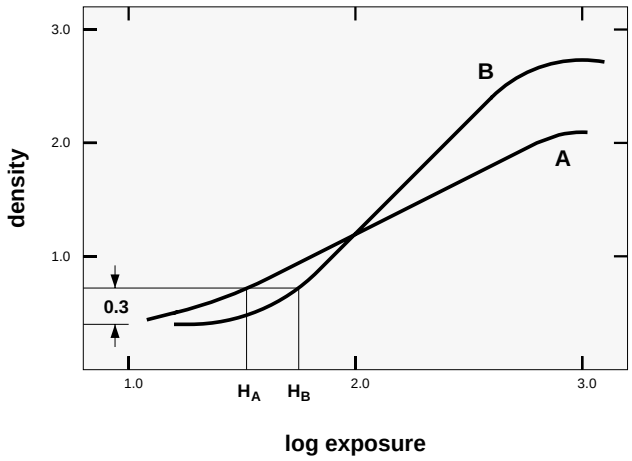

Figure 2.14: Concept of speed.

2.2.5 Resolving Power

The image quality is directly related to the size and distribution of the silver halide crystals and the dyes suspended in the emulsion. The crystals are also called *corn*, and the corn size corresponds to the diameter of the crystal. *Granularity* refers to the size and distribution, *concentration* to the amount of light-sensitive material per unit volume. Emulsions are usually classified as fine-, medium-, or coarse-grained.

The resolving power of an emulsion refers to the number of alternating bars and spaces of equal width which can be recorded as visually separate elements in the space of one millimeter. A bar and a space is called a line or line pair. A resolving power of 50 l/mm means that 50 bars, separated by 50 spaces, can be discerned per millimeter. Fig. 2.15 shows a typical test pattern used to determine the resolving power.

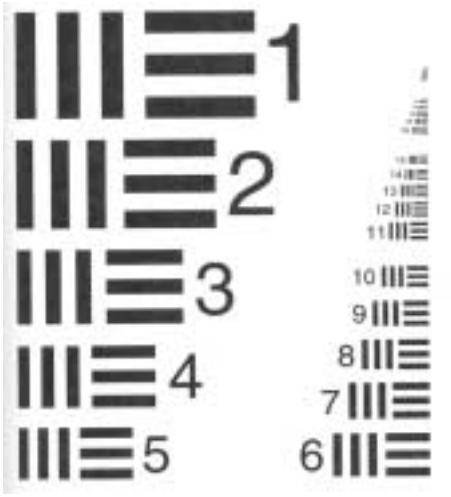

Figure 2.15: Typical test pattern (three-bar target) for determining resolving power.

The three-bar target shown in Fig. 2.15 is photographed under laboratory conditions using a diffraction-limited objective with large aperture (to reduce the effect of the optical system on the resolution). The resolving power is highly dependent on the target contrast. Therefore, targets with different contrast are used. High contrast targets have perfectly black bars, separated by white spaces, whereas lower contrast targets have bars and spaces with varying grey shades. In the Table below are listed some aerial films with their resolving powers.

Note that there is an inverse relationship between speed and resolving power: coarse-grained films are fast but have a lower resolution than fine-grained aerial films.

Table 2.3: Films for aerial photography

.

manufacturer	*designation*	*speed (AFS)*	*resolution [l/mm]*		*gamma*
			contrast 1000 : 1	*contrast 1.6 : 1*	
Agfa	Aviophot Pan		133		1.0 - 1.4
Kodak	Plus-X Aerographic	160	100	50	1.3
Kodak	High Definition	6.4	630	250	1.3
Kodak	Infrared Aerographic	320	80	40	2.3
Kodak	Aerial Color	6	200	100	

Chapter 3

Digital Cameras

3.1 Overview

The popular term “digital camera" is rather informal and may even be misleading because the output is in many cases an analog signal. An more generic term is *solid-state camera*.

Other frequently used terms include *CCD camera* and *solid-state camera*. Though these terms obviously refer to the type of sensing elements, they are often used in a more generic sense.

The chief advantage of digital cameras over the classical film-based cameras is the instant availability of images for further processing and analysis. This is essential in real-time applications (e.g. robotics, certain industrial applications, bio-mechanics, etc.).

Another advantage is the increased spectral flexibility of digital cameras. The major drawback is the limited resolution or limited field of view.

Digital cameras have been used for special photogrammtric applications since the early seventies. However, vidicon-tube cameras available at that time were not very accurate because the imaging tubes were not stable. This disadvantage was eliminated with the appearance of solid-state cameras in the early eighties. The charge-coupled device provides high stability and is therefore the preferred sensing device in today’s digital cameras.

The most distinct characteristic of a digital camera is the image sensing device. Because of its popularity we restrict the discussion to solid-state sensors, in particular to charge coupled devices (CCD).

The sensor is glued to a ceramic substrate and covered by a glass. Typical chip sizes are 1/2 and 2/3 inches with as many as 2048×2048 sensing elements. However, sensors with fewer than $1K \times 1K$ elements are more common. Fig. 3.1 depicts a line sensor (a) and a 2D sensor chip (b).

The dimension of a sensing element is smaller than $10 \quad \mu$m, with an insulation space of a few microns between them. This can easily be verified when considering the physical dimensions of the chip and the number of elements.

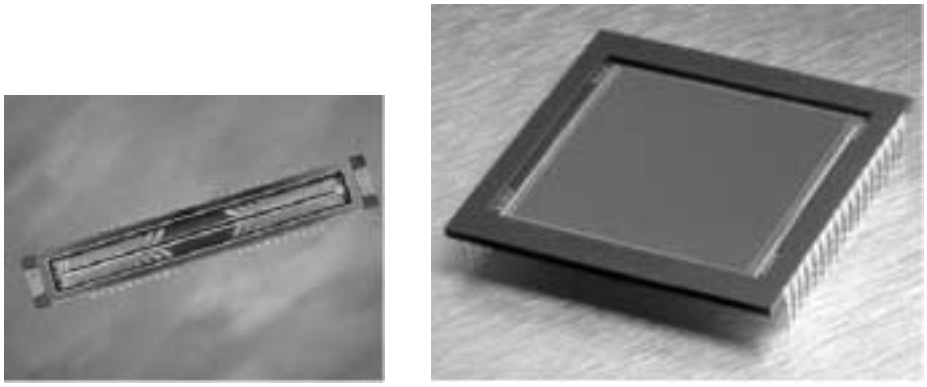

Figure 3.1: Example of 1D sensor element and 2D array sensor.

3.1.1 Camera Overview

Fig. 3.2 depicts a functional block diagram of the major components of a solid-state camera.

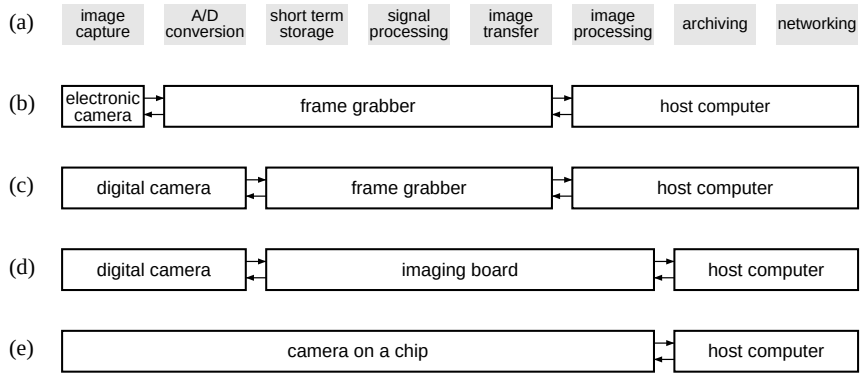

Figure 3.2: Functional block diagram of a solid-state camera. A real camera may not have all components. The diagram is simplified, e.g. external signals received by the camera are not shown.

The optics component includes lens assembly and filters, such as an infrared blocking

filter to limit the spectral response to the visible spectrum. Many cameras use a C-mount for the lens. Here, the distance between mount and image plane is 17.526 mm. As an option, the optics subsystem may comprise a shutter.

The most distinct characteristic of an electronic camera is the image sensing device. Section 3.2 provides an overview of charge-coupled devices.

The solid-state sensor, positioned in the image plane, is glued on a ceramic substrate. The sensing elements (pixels) are either arranged in a linear array or a frame array. Linear arrays are used for aerial cameras while close range applications, including mobile mapping systems, employ frame array cameras.

The accuracy of a solid-state camera depends a great deal on the accuracy and stability of the sensing elements, for example on the uniformity of the sensor element spacing and the flatness of the array. From the manufacturing process we can expect an accuracy of $1/10^{th}$ of a micron. Considering a sensor element, size 10 μm, the regularity amounts to $1/100$. Camera calibration and measurements of the position and the spacing of sensor elements confirm that the regularity is between $1/50^{th}$ and $1/100^{th}$ of the spacing.

The voltage generated by the sensor's read out mechanism must be amplified for further processing, which begins with converting the analog signal to a digital signal. This is not only necessary for producing a digital output, but also for signal and image processing. The functionality of these two components may range from rudimentary to very sophisticated in a real camera.

You may consider the first two components (optics and solid-state sensor) as image capture, the amplifiers and ADC as image digitization, and signal and image processing as image restoration. A few examples illustrate the importance of image restoration. The dark current can be measured and subtracted so that only its noise signal component remains; defective pixels can be determined and an interpolated signal can be output; the contrast can be changed (Gamma correction); and image compression may be applied. The following example demonstrates the need for data compression.

3.1.2 Multiple frame cameras

The classical film-based cameras used in photogrammetry are often divided into aerial and terrestrial (close-range) cameras. The same principle can be applied for digital cameras. A digital aerial camera with a resolution comparable to a classical frame camera must have on the order of $15,000 \times 15,000$ sensing elements. Such image sensors do not (yet) exist. Two solutions exist to overcome this problem: *line cameras* and *multiple cameras*, housed in one camera body.

Fig. 3.3 shows an example of a multi-camera system (UltraCam from Vexcel). It consists of 8 different cameras that are mounted in a common camera frame. The ground coverage of each of these frame cameras slightly overlaps and the 8 different images are merged together to one uniform frame image by way of image processing.

3.1.3 Line cameras

An alternative solution to frame cameras are the so called *line cameras* of which the *3-line camera* is the most popular one. The 3-line camera employs three linear areas

Figure 3.3: Example of a multi-camera system (Vexcel UltraCam), consisting of 8 different cameras that are mounted in a slightly convergent mode to assure overlap of the individual images.

which are mounted in the image plane in fore, nadir and aft position (see Fig. 3.4(a). With this configuration, triple coverage of the surface is obtained. Examples of 3-line cameras include Leica's ADS40. It is also possible to implement the multiple line concept by having convergent lenses for every line, as depicted in Fig. 3.4(b).

A well-known example of a one line-camera is SPOT. The linear array consists of 7,000 sensing elements. Stereo is obtained by overlapping strips obtained from adjacent orbits.

Fig. 3.5 shows the overlap configuration obtained with a 3-Line camera.

3.1.4 Camera Electronics

The camera electronics contains the power supply, a video timing and a sensor clock generator. Additional components are dedicated to special signal processing tasks, such as noise reduction, high frequency cross-talk removal and black level stabilization. A "true" digital camera would have an analog-to-digital converter which samples the video signal with the frequency of the sensor element clock.

The camera electronics may have additional components which serve the purpose to increase the camera's functionality. An example is the acceptance of external sync which allows to synchronize the camera with other devices. This would allow for multiple camera setups with uniform sync.

Cameras with mechanical (or LCD) shutters need appropriate electronics to read

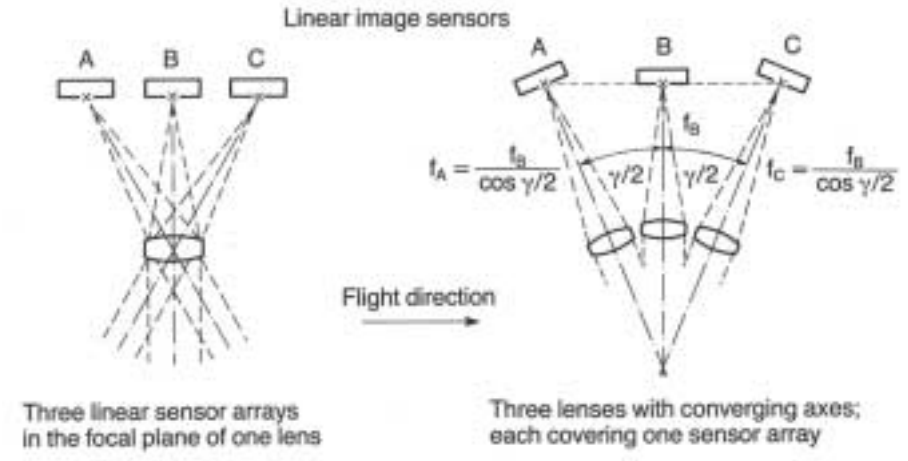

Figure 3.4: Schematic diagram of a 3-line camera. In (a), 3 sensor lines are mounted on the image plane in fore, nadir and aft locations. An alternative solution is using 3 convergent cameras, each with a single line mounted in the center (b).

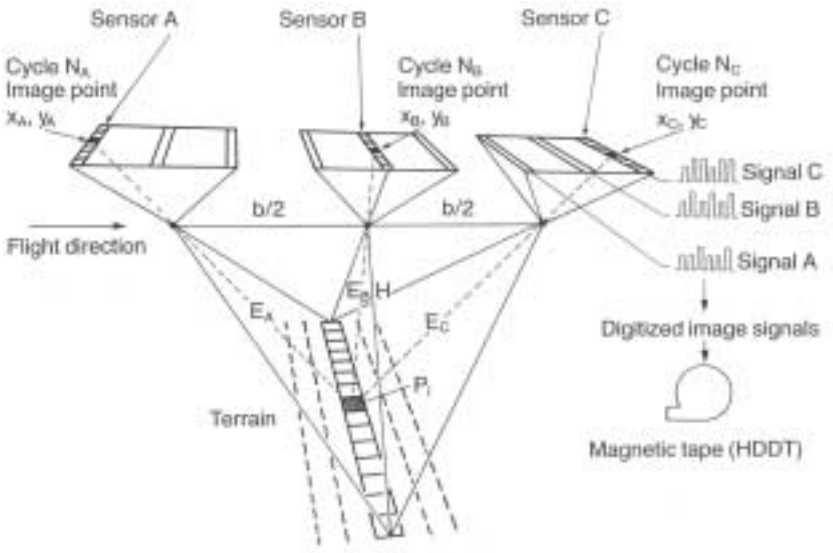

Figure 3.5: Stereo obtained with a 3-Line camera.

external signals to trigger the shutter.

3.1.5 Signal Transmission

The signal transmission follows the video standards. Unfortunately, there is no such thing as a uniform video standard used worldwide. The first standard dates back to 1941 when the National Television Systems Committee (NTSC) defined RS-170 for black-and-white television. This standard is used in North America, parts of South America, in Japan and the Philippines. European countries developed other standards, e.g. PAL (phase alternate line) and SECAM (sequential color and memory). Yet another standard for black-and-white television was defined by CCIR (Commité Consultatif International des Radiocommunications). It differs only slightly to the NTSC standard, however.

Both, the R-170 and CCIR standard use the principle of interlacing. Here, the image, called a frame, consists of two fields. The odd field contains the odd line numbers, the even field the even line numbers. This technique is known from video monitors.

3.1.6 Frame Grabbers

Frame grabbers receive the video signal, convert it, buffer data and output it to the storage device of the digital image. The analog front end of a frame grabber preprocesses the video signal and passes it to the AD converter. The analog front end must cope with different signals (e.g. different voltage level and impedance).

3.2 CCD Sensors: Working Principle and Properties

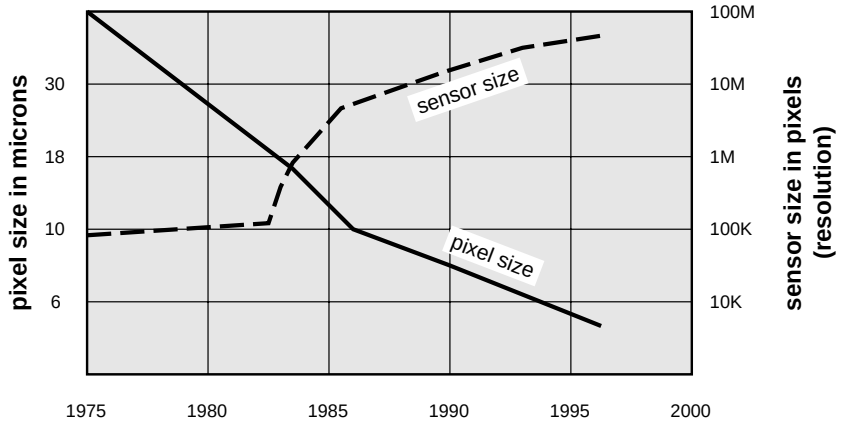

Figure 3.6: Development of CCD arrays over a period of 25 years.

The *charge-coupled device (CCD)* was invented in 1970. The first CCD line sensor contained 96 pixels; today, chips with over 50 million pixels are commercially available.

Fig. 3.6 on the preceding page illustrates the astounding development of CCD sensors over a period of 25 years. The sensor size in pixels is usually loosely termed *resolution*, giving rise to confusion since this term has a different meaning in photogrammetry[1].

3.2.1 Working Principle

Fig. 3.7(a) is a schematic diagram of a semiconductor capacitor—the basic building block of a CCD. The semiconductor material is usually silicon and the insulator is an oxide (MOS capacitor). The metal electrodes are separated from the semiconductor by the insulator. Applying a positive voltage at the electrode forces the mobile holes to move toward the electric ground. In this fashion, a region (depletion region) with no positive charge forms below the electrode on the opposite side of the insulator.

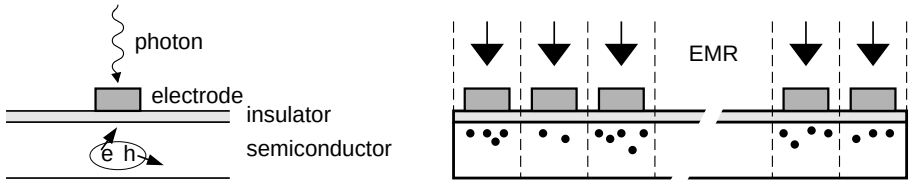

Figure 3.7: Schematic diagram of CCD detector. In (a) a photon with an energy greater than the bandgap of the semiconductor generates an electron-hole pair. The electron e is attracted by the positive voltage of the electrode while the mobile hole moves toward the ground. The collected electrons together with the electrode form a capacitor. In (b) this basic arrangement is repeated many times to form a linear array.

Suppose EMR is incident on the device. Photons with an energy greater than the band gap energy of the semiconductor may be absorbed in the depletion region, creating an electron-hole pair. The electron—referred to as *photon electron*—is attracted by the positive charge of the metal electrode and remains in the depletion region while the mobile hole moves toward the electrical ground. As a result, a charge accumulates at opposite sides of the insulator. The maximum charge depends on the voltage applied to the electrode. Note that the actual charge is proportional to the number of absorbed photons under the electrode.

The band gap energy of silicon corresponds to the energy of a photon with a wavelength of 1.1 μm. Lower energy photons (but still exceeding the band gap) may penetrate the depletion region and be absorbed outside. In that case, the generated electron-hole pair may recombine before the electron reaches the depletion region. We realize that not every photon generates an electron that is accumulated at the capacitor site. Consequently, the quantum efficiency is less than unity.

[1]Resolution refers to the minimum distance between two adjacent features, or the minimum size of a feature, which can be detected by photogrammetric data acquisition systems. For photography, this distance is usually expressed in line pairs per millimeter (lp/mm).

An ever increasing number of capacitors are arranged into what is called a *CCD array*. Fig. 3.7(b) illustrates the concept of a one-dimensional array (called a linear array) that may consist of thousands of capacitors, each of which holds a charge proportional to the irradiance at each site. It is customary to refer to these capacitor sites as *detector pixels*, or pixels for short. Two-dimensional pixel arrangements in rows and columns are called full-frame or staring arrays.

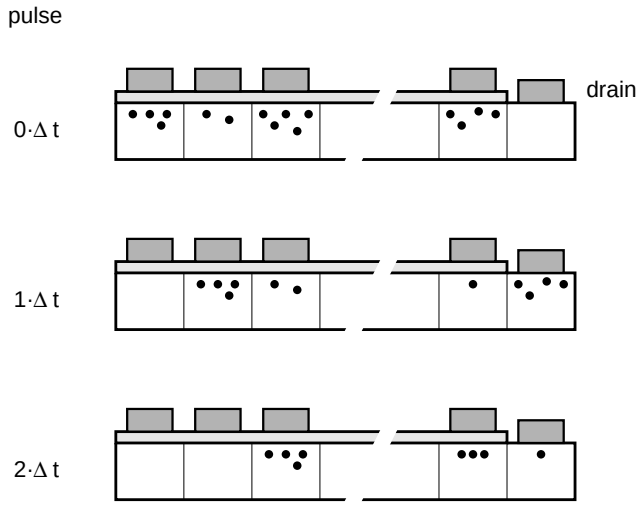

Figure 3.8: Principle of charge transfer. The top row shows a linear array of accumulated charge packets. Applying a voltage greater than V_1 of electrode 1 momentarily pulls charge over to the second electrode (middle row). Repeating this operation in a sequential fashion eventually moves all packets to the final electrode (drain) where the charge is measured.

The next step is concerned with transferring and measuring the accumulated charge. The principle is shown in Fig. 3.8. Suppose that the voltage of electrode i+1 is momentarily made larger than that of electrode i. In that case, the negative charge under electrode i is pulled over to site i+1, below electrode i+1, provided that adjacent depletion regions overlap. Now, a sequence of voltage pulses will cause a sequential movement of the charges across all pixels to the drain (last electrode) where each packet of charge can be measured. The original location of the pixel whose charge is being measured in the drain is directly related to the time when a voltage pulse was applied.

Several ingenious solutions for transferring the charge accurately and quickly have been developed. It is beyond the scope of this book to describe the transfer technology in any detail. The following is a brief summary of some of the methods.

3.2.2 Charge Transfer

Linear Array With Bilinear Readout

As sketched in Fig. 3.9, a linear array (CCD shift register) is placed on both sides of the single line of detectors. Since these two CCD arrays are also light sensitive, they must be shielded. After integration, the charge accumulated in the active detectors is transferred to the two shift registers during one clock period. The shift registers are read out in a serial fashion as described above. If the readout time is equal to the integration time, then this sensor may operate continuously without a shutter. This principle, known as *push broom*, is put to advantage in line cameras mounted on moving platforms to provide continuous coverage of the object space.

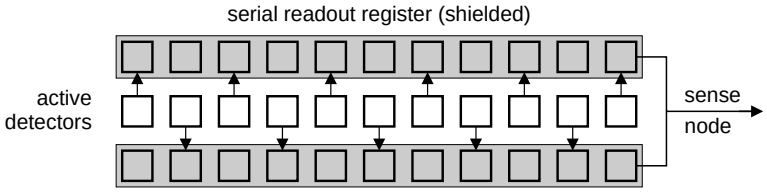

Figure 3.9: Principle of linear array with bilinear readout. The accumulated charge is transferred during one pixel clock from the active detectors to the adjacent shift registers, from where it is read out sequentially.

Frame Transfer

You can visualize a frame transfer imager as consisting of two identical arrays. The active array accumulates charges during integration time. This charge is then transferred to the storage array, which must be shielded since it is also light sensitive. During the transfer, charge is still accumulating in the active array, causing a slightly smeared image.

The storage array is read out serially, line by line. The time necessary to read out the storage array far exceeds the integration. Therefore, this architecture requires a mechanical shutter. The shutter offers the advantage that the smearing effect is suppressed.

Interline Transfer

Fig. 3.10 on the following page illustrates the concept of interline transfer arrays. Here, the columns of active detectors (pixels) are separated by vertical transfer registers. The accumulated charge in the pixels is transferred at once and then read out serially. This again allows an open shutter operation, assuming that the read out time does not exceed the integration time.

Since the CCD detectors of the transfer register are also sensitive to irradiance, they must be shielded. This, in turn, reduces the effective irradiance over the chip area. The effective irradiance is often called *fill factor*. The interline transfer imager as described

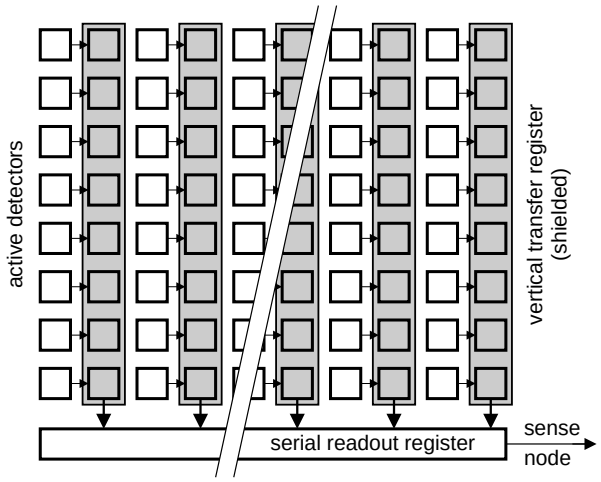

Figure 3.10: Principle of linear array with bilinear readout. The accumulated charge is transferred during one pixel clock from the active detectors to the adjacent shift registers from where it is read out sequentially.

here has a fill factor of 50%. Consequently, longer integration times are required to capture an image. To increase the fill factor, microlenses may be used. In front of every pixel is a lens that directs the light incident on an area defined by adjacent active pixels to the (smaller) pixel.

3.2.3 Spectral Response

Silicon is the most frequently used semiconductor material. In an ideal silicon detector, every photon exceeding the band gap ($\lambda < 1.1$ μm) causes a photon electron that is collected and eventually measured. The quantum efficiency is unity and the spectral response is represented by a step function. As indicated in Fig. 3.11, the quantum efficiency of a real CCD sensor is less than unity for various reasons. For one, not all the incident flux interacts with the detector (e.g. reflected by the electrode in front illuminated sensors). Additionally, some electron-hole pairs recombine. Photons with longer wavelengths penetrate the depletion region and cause electron-hole pairs deep inside the silicon. Here, the probability of recombination is greater and many fewer electrons are attracted by the capacitor. The drop in spectral response toward blue and UV is also related to the electrode material that may become opaque for $\lambda < 0.4$ μm.

Sensors illuminated from the back avoid diffraction and reflection problems caused by the electrode. Therefore, they have a higher quantum efficiency than front illuminated sensors. However, the detector must be thinner, because high energy photons are absorbed near the surface—opposite the depletion region—and the chances of electron/hole recombination are lower with shorter diffusion length.

In order to make the detector sensitive to other spectral bands (mainly IR), detector

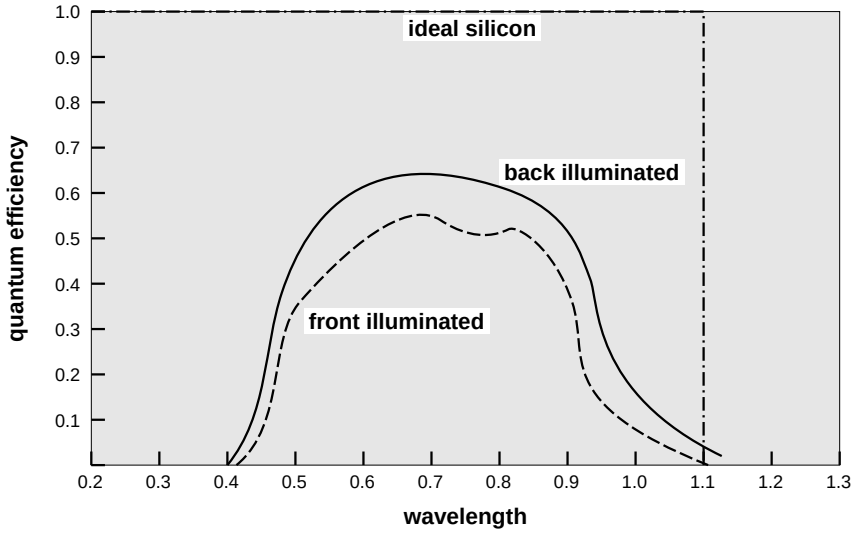

Figure 3.11: Spectral response of CCD sensors. In an ideal silicon detector all photons exceeding the band gap energy generate electrons. Front illuminated sensors have a lower quantum efficiency than back illuminated sensors because part of the incident flux may be absorbed or redirected by the electrodes (see text for details).

material with the corresponding bandgap energy must be selected. This leads to hybrid CCD arrays where the semiconductor and the CCD mechanism are two separate components.

Chapter 4

Properties of Aerial Photography

4.1 Introduction

Aerial photography is the basic data source for making maps by photogrametric means. The photograph is the end result of the data acquisition process discussed in the previous chapter. Actually, the net result of any photographic mission are the photographic negatives. Of prime importance for measuring and interpretation are the positive reproductions from the negatives, called *diapositives*.

Many factors determine the quality of aerial photography, such as

- design and quality of lens system
- manufacturing the camera
- photographic material
- development process
- weather conditions and sun angle during photo flight

In this chapter we describe the types of aerial photographs, their geometrical properties and relationship to object space.

4.2 Classification of aerial photographs

Aerial photographs are usually classified according to the orientation of the camera axis, the focal length of the camera, and the type of emulsion.

4.2.1 Orientation of camera axis

Here, we introduce the terminology used for classifying aerial photographs according to the orientation of the camera axis. Fig. 4.1 illustrates the different cases.

true vertical photograph A photograph with the camera axis perfectly vertical (identical to plumb line through exposure center). Such photographs hardly exist in reality.

near vertical photograph A photograph with the camera axis nearly vertical. The deviation from the vertical is called tilt. It must not exceed mechanical limitations of stereoplotter to accomodate it. Gyroscopically controlled mounts provide stability of the camera so that the tilt is usually less than two to three degrees.

oblique photograph A photograph with the camera axis intentially tilted between the vertical and horizontal. A **high oblique photograph**, depicted in Fig. 4.1(c) is tilted so much that the horizon is visible on the photograph. A **low oblique** does not show the horizon (Fig. 4.1(b)).

The total area photographed with obliques is much larger than that of vertical photographs. The main application of oblique photographs is in reconnaissance.

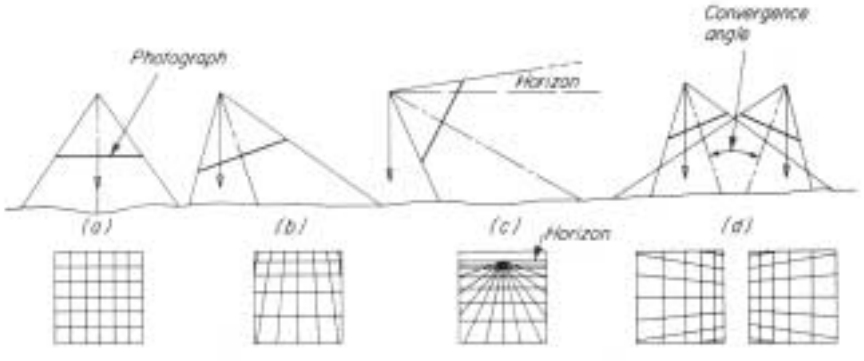

Figure 4.1: Classification of photographs according to camera orientation. In (a) the schematic diagram of a true vertical photograph is shown; (b) shows a low oblique and (c) depicts a high oblique photograph.

4.2.2 Angular coverage

The angular coverage is a function of focal length and format size. Since the format size is almost exclusively $9'' \times 9''$ the angular coverage depends on the focal length of the camera only. Standard focal lengths and associated angular coverages are summarized in Table 4.1.

Table 4.1: Summary of photographs with different angular coverage.

	super-wide	wide-angle	inter-mediate	normal-angle	narrow-angle
focal length [mm]	85.	157.	210.	305.	610.
angular coverage [o]	119.	82.	64.	46.	24.

4.2.3 Emulsion type

The sensitivity range of the emulsion is used to classify photography into

panchromatic black and white This is most widely used type of emulsion for photogrammetric mapping.

color Color photography is mainly used for interpretation purposes. Recently, color is increasingly being used for mapping applications.

infrared black and white Since infrared is less affected by haze it is used in applications where weather conditions may not be as favorable as for mapping missions (e.g. intelligence).

false color This is particular useful for interpretation, mainly for analyzing vegetation (e.g. crop desease) and water pollution.

4.3 Geometric properties of aerial photographs

We restrict the discussion about geometric properties to frame photography, that is, photographs exposed in one instant. Furthermore, we assume central projection.

4.3.1 Definitions

Fig. 4.2 shows a diapositive in near vertical position. The following definitions apply:

perspective center *C* calibrated perspective center (see also camera calibration, interior orientation).

focal length *c* calibrated focal length (see also camera calibration, interior orientation).

principal point *PP* principal point of autocollimation (see also camera calibration, interior orienttion).

camera axis *C*-*PP* axis defined by the projection center C and the principal point *PP*. The camera axis represents the optical axis. It is perpendicular to the image plane

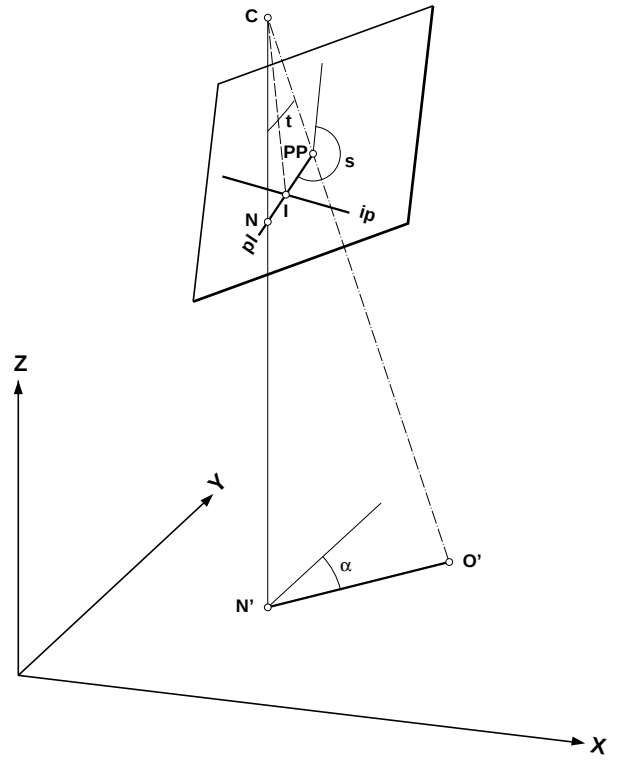

Figure 4.2: Tilted photograph in diapositive position and ground control coordinate system.

nadir point N' also called photo nadir point, is the intersection of vertical (plumb line) from perspective center with photograph.

ground nadir point N intersection of vertical from perspective center with the earth's surface.

tilt angle t angle between vertical and camera axis.

swing angle s is the angle at the principal point measured from the $+$*y-axis* counterclockwise to the nadir N.

azimut α is the angle at the ground nadir N measured from the $+$*Y-axis* in the ground system counterclockwise to the intersection O of the camera axis with the ground surface. It is the azimut of the trace of the principal plane in the XY-plane of the ground system.

principal line *pl* intersection of plane defined by the vertical through perspective center and camera axis with the photograph. Both, the nadir N and the principal point

PP are on the principal line. The principal line is oriented in the direction of steepest inclination of of the tilted photograph.

isocenter I is the intersection of the bisector of angle t with the photograph. It is on the principal line.

isometric parallel *ip* is in the plane of photograph and is perpendicular to the principal line at the isocenter.

true horizon line intersection of a horizontal plane through persepective center with photograph or its extension. The horizon line falls within the extent of the photograph only for high oblique photographs.

horizon point intersection of principal line with true horizon line.

4.3.2 Image and object space

The photograph is a *perspective (central) projection*. During the image formation process, the physical projection center object side is the center of the entrance pupil while the center of the exit pupil is the projection center image side (see also Fig. 4.3. The two projection centers are separated by the *nodal separation*. The two projection centers also separate the space into *image space* and *object space* as indicated in Fig. 4.3.

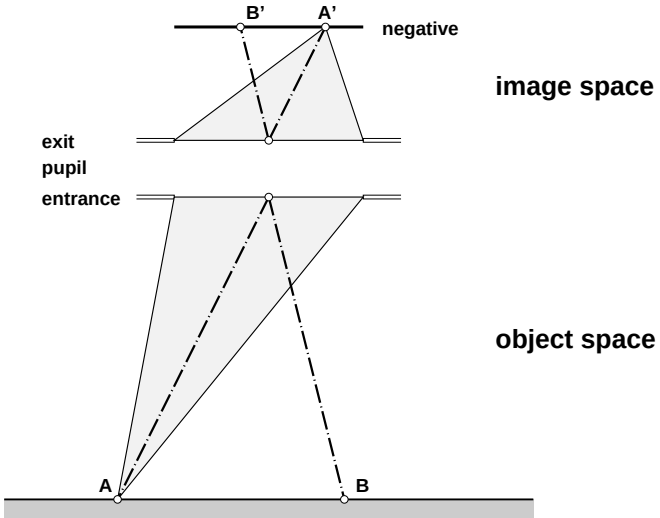

Figure 4.3: The concept of image and object space.

During the camera calibration process the projection center in image space is changed to a new position, called the calibrated projection center. As discussed in 2.6, this is necessary to achieve close similarity between the image and object bundle.

4.3.3 Photo scale

We use the representative fraction for scale expressions, in form of a ratio, e.g. 1 : 5,000. As illustrated in Fig. 4.4 the scale of a near vertical photograph can be approximated by

$$m_b = \frac{c}{H} \tag{4.1}$$

where m_b is the *photograph scale number*, c the calibrated focal length, and H the *flight height* above mean ground elevation. Note that the flight height H refers to the average ground elevation. If it is with respect to the datum, then it is called *flight altitude* H_A, with $H_A = H + h$.

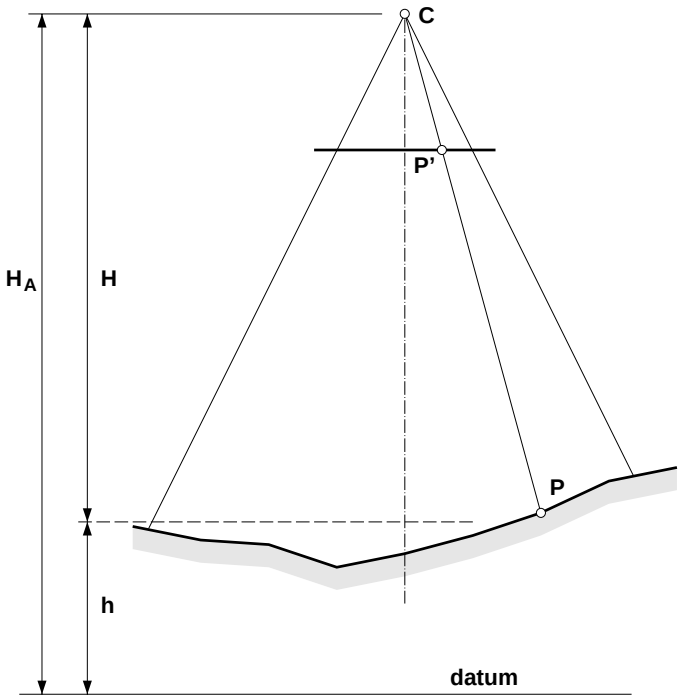

Figure 4.4: Flight height, flight altitude and scale of aerial photograph.

The photograph scale varies from point to point. For example, the scale for point P can easily be determined as the ratio of image distance CP' to object distance CP by

$$m_P = \frac{CP'}{CP} \tag{4.2}$$

$$CP\prime = \sqrt{x_P^2 + y_P^2 + c^2} \tag{4.3}$$

$$CP = \sqrt{(X_P - X_C)^2 + (Y_P - Y_C)^2 + (Z_P - Z_C)^2} \tag{4.4}$$

where x_P, y_P are the photo-coordinates, X_P, Y_P, Z_P the ground coordinates of point P, and X_C, Y_C, Z_C the coordinates of the projection center C in the ground coordinate system. Clearly, above equation takes into account any tilt and topographic variations of the surface *(relief)*.

4.3.4 Relief displacement

The effect of relief does not only cause a change in the scale but can also be considered as a component of image displacement. Fig. 4.5 illustrates this concept. Suppose point T is on top of a building and point B at the bottom. On a map, both points have identical X, Y coordinates; however, on the photograph they are imaged at different positions, namely in T' and B'. The distance d between the two photo points is called *relief displacement* because it is caused by the elevation difference Δh between T and B.

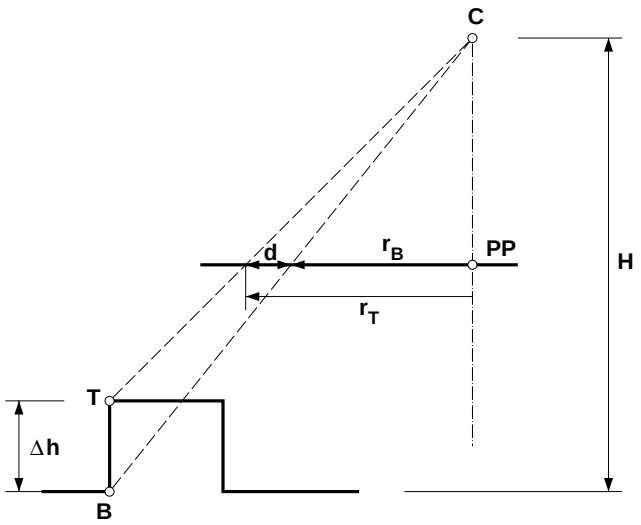

Figure 4.5: Relief displacement.

The magnitude of relief displacement for a true vertical photograph can be determined by the following equation

$$d = \frac{r\ \Delta h}{H} = \frac{r'\ \Delta h}{H - \Delta h} \tag{4.5}$$

where $r = \sqrt{x_T^2 + y_T^2}$, $r' = \sqrt{x_B^2 + y_B^2}$, and Δh the elevation difference of two points on a vertical. Eq. 4.5 can be used to determine the elevation Δh of a vertical object

$$h = \frac{d\ H}{r} \tag{4.6}$$

The direction of relief displacement is radial with respect to the nadir point N', independent of camera tilt.

Chapter 5

Elements of Analytical Photogrammetry

5.1 Introduction, Concept of Image and Object Space

Photogrammetry is the science of obtaining reliable information about objects and of measuring and interpreting this information. The task of obtaining information is called data acquisition, a process we discussed at length in GS601, Chapter 2. Fig. 5.1(a) depicts the data acquisition process. Light rays reflected from points on the object, say from point A, form a divergent bundle which is transformed to a convergent bundle by the lens. The principal rays of each bundle of all object points pass through the center of the entrance and exit pupil, unchanged in direction. The front and rear nodal points are good approximations for the pupil centers.

Another major task of photogrammetry is concerned with reconstructing the object space from images. This entails two problems: geometric reconstruction (e.g. the position of objects) and radiometric reconstruction (e.g. the gray shades of a surface). The latter problem is relevant when photographic products are generated, such as orthophotos. Photogrammetry is mainly concerned with the geometric reconstruction. The object space is only partially reconstructed, however. With partial reconstruction we mean that only a fraction of the information recorded from the object space is used for its representation. Take a map, for example. It may only show the perimeter of buildings, not all the intricate details which make up real buildings.

Obviously, the success of reconstruction in terms of geometrical accuracy depends largely on the similarity of the image bundle compared to the bundle of principal rays that entered the lens during the instance of exposure. The purpose of camera calibration is to define an image space so that the similarity becomes as close as possible.

The geometrical relationship between image and object space can best be established by introducing suitable coordinate systems for referencing both spaces. We describe the coordinate systems in the next section. Various relationships exist between image and object space. In Table 5.1 the most common relationships are summarized, together with the associated photogrammetric procedures and the underlying mathematical models.

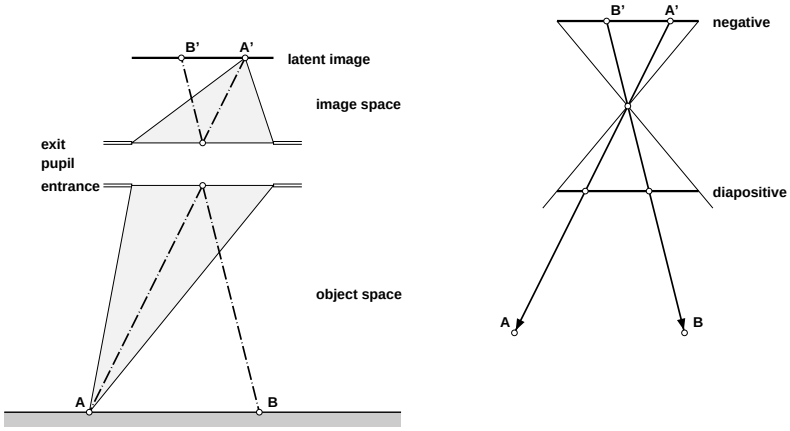

Figure 5.1: In (a) the data acquisition process is depicted. In (b) we illustrate the reconstruction process.

In this chapter we describe these procedures and the mathematical models, except aerotriangulation (block adjustment) which will be treated later. For one and the same procedure, several mathematical models may exist. They differ mainly in the degree of complexity, that is, how closely they describe physical processes. For example, a similarity transformation is a good approximation to describe the process of converting measured coordinates to photo-coordinates. This simple model can be extended to describe more closely the underlying measuring process. With a few exceptions, we will not address the refinement of the mathematical model.

5.2 Coordinate Systems

5.2.1 Photo-Coordinate System

The photo-coordinate system serves as the reference for expressing spatial positions and relations of the image space. It is a 3-D cartesian system with the origin at the perspective center. Fig. 5.2 depicts a diapositive with fiducial marks that define the fiducial center *FC*. During the calibration procedure, the offset between fiducial center and principal point of autocollimation, *PP*, is determined, as well as the origin of the radial distortion, *PS*. The x, y coordinate plane is parallel to the photograph and the positive $x-$axis points toward the flight direction.

Positions in the image space are expressed by point vectors. For example, point vector $\mathbf{p}$ defines the position of point P on the diapositive (see Fig. 5.2). Point vectors of positions on the diapositive (or negative) are also called *image vectors*. We have for point P

Table 5.1: Summary of the most important relationships between image and object space.

relationship between	*procedure*	*mathematical model*
measuring system and photo-coordinate system	interior orientation	2-D transformation
photo-coordinate system and object coordinate system	exterior orientation	collinearity eq.
photo-coordinate systems of a stereopair	relative orientation	collinearity eq. coplanarity condition
model coordinate system and object coordinate system	absolute orientation	7-parameter transformation
several photo-coordinate systems and object coordinate system	bundle block adjustment	collinearity eq.
several model coordinate systems and object coordinate system	independent model block adjustment	7 parameter transformation

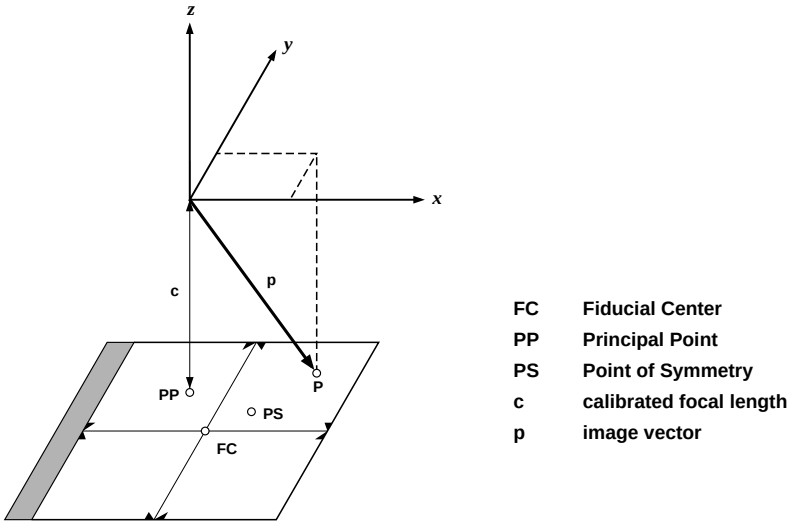

Figure 5.2: Definition of the photo-coordinate system.

$$\mathbf{p} = \begin{bmatrix} x_p \\ y_p \\ -c \end{bmatrix} \tag{5.1}$$

Note that for a diapositive the third component is negative. This changes to a positive

value in the rare case a negative is used instead of a diapositive.

5.2.2 Object Space Coordinate Systems

In order to keep the mathematical development of relating image and object space simple, both spaces use 3-D cartesian coordinate systems. Positions of control points in object space are likely available in another coordinate systems, e.g. State Plane coordinates. It is important to convert any given coordinate system to a cartesian system before photogrammetric procedures, such as orientations or aerotriangulation, are performed.

5.3 Interior Orientation

We have already introduced the term *interior orientation* in the discussion about camera calibration (see GS601, Chapter 2), to define the metric characteristics of aerial cameras. Here we use the same term for a slightly different purpose. From Table 5.1 we conclude that the purpose of interior orientation is to establish the relationship between a measuring system[1] and the photo-coordinate system. This is necessary because it is not possible to measure photo-coordinates directly. One reason is that the origin of the photo-coordinate system is only mathematically defined; since it is not visible it cannot coincide with the origin of the measuring system.

Fig. 5.3 illustrates the case where the diapositive to be measured is inserted in the measuring system whose coordinate axis are xm, ym. The task is to determine the transformation parameters so that measured points can be transformed into photo-coordinates.

5.3.1 Similarity Transformation

The most simple mathematical model for interior orientation is a similarity transformation with the four parameters: translation vector **t**, scale factor s, and rotation angle α.

$$xf = s(xm\ \cos(\alpha) - ym\ \sin(\alpha)) - xt \tag{5.2}$$
$$yf = s(xm\ \sin(\alpha) + ym\ \cos(\alpha)) - yt \tag{5.3}$$

These equations can also be written in the following form:

$$xf = a_{11}xm - a_{12}ym - xt \tag{5.4}$$
$$yf = a_{12}xm + a_{11}ym - yt \tag{5.5}$$

If we consider a_{11}, a_{12}, xt, yt as parameters, then above equations are linear in the parameters. Consequently, they can be directly used as observation equations for a least-squares adjustment. Two observation equations are formed for every point known in

[1] Measuring systems are discussed in the next chapter.

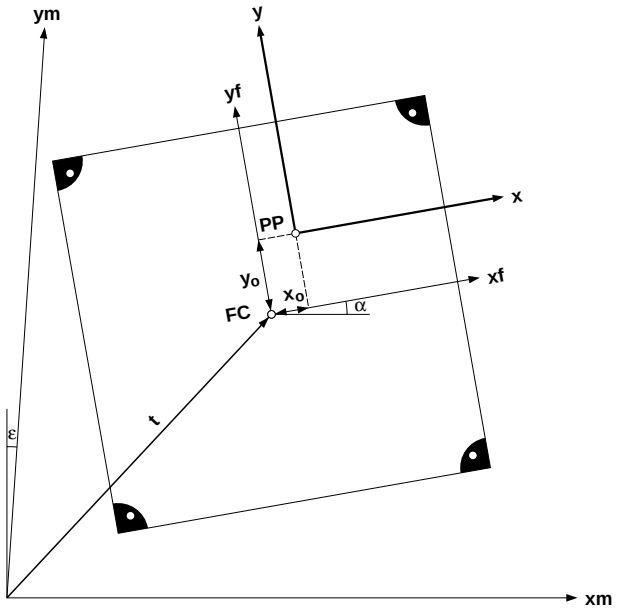

Figure 5.3: Relationship between measuring system and photo-coordinate system.

both coordinate systems. Known points in the photo-coordinate system are the fiducial marks. Thus, computing the parameters of the interior orientation amounts to measuring the fiducial marks (in the measuring system).

Actually, the fiducial marks are known with respect to the fiducial center. Therefore, the process just described will determine parameters with respect to the *fiducial coordinate system xf, yf*. Since the origin of the photo-coordinate system is known in the fiducial system (x_0, y_0), the photo-coordinates are readily obtained by the translation

$$x = xf - x_0 \quad (5.6)$$
$$y = yf - y_0 \quad (5.7)$$

5.3.2 Affine Transformation

The affine transformation is an improved mathematical model for the interior orientation because it more closely describes the physical reality of the measuring system. The parameters are two scale factors s_x, s_y, a rotation angle α, a skew angle ϵ, and a translation vector $\mathbf{t} = [xt, yt]^T$. The measuring system is a manufactured product and, as such, not perfect. For example, the two coordinate axis are not exactly rectangular,

as indicated in Fig. 5.3(b). The skew angle expresses the nonperpendicularity. Also, the scale is different between the the two axis.

We have

$$xf = a_{11}xm + a_{12}ym - xt \quad (5.8)$$
$$yf = a_{21}xm + a_{22}ym - yt \quad (5.9)$$

where

a_{11} $s_x(\cos(\alpha - \epsilon\sin(\alpha))$
a_{12} $-s_y(\sin(\alpha))$
a_{21} $s_x(\sin(\alpha + \epsilon\cos(\alpha))$

Eq. 4.8 and 5.9 are also linear in the parameters. Like in the case of a similarity transformation, these equations can be directly used as observation equations. With four fiducial marks we obtain eight equations leaving a redundancy of two.

5.3.3 Correction for Radial Distortion

As discussed in GS601 Chapter 2, radial distortion causes off-axial points to be radially displaced. A positive distortion increases the lateral magnification while a negative distortion reduces it.

Distortion values are determined during the process of camera calibration. They are usually listed in tabular form, either as a function of the radius or the angle at the perspective center. For aerial cameras the distortion values are very small. Hence, it suffices to linearly interpolate the distortion. Suppose we want to determine the distortion for image point x_p, y_p. The radius is $r_p = (x_p^2 + y_p^2)^{1/2}$. From the table we obtain the distortion dr_i for $r_i < r_p$ and dr_j for $r_j > r_p$. The distortion for r_p is interpolated

$$dr_p = \frac{(dr_j - dr_i)\, r_p}{(r_j - r_i)} \quad (5.10)$$

As indicated in Fig. 5.4 the corrections in x- and y-direction are

$$dr_x = \frac{x_p}{r_p} dr_p \quad (5.11)$$
$$dr_y = \frac{y_p}{r_p} dr_p \quad (5.12)$$

Finally, the photo-coordinates must be corrected as follows:

$$x_p = x_p - dr_x = x_p(1 - \frac{dr_p}{r_p}) \quad (5.13)$$
$$y_p = y_p - dr_y = y_p(1 - \frac{dr_p}{r_p}) \quad (5.14)$$

The radial distortion can also be represented by an odd-power polynomial of the form

$$dr = p_0\, r + p_1\, r^3 + p_2\, r^5 + \cdots \tag{5.15}$$

The coefficients p_i are found by fitting the polynomial curve to the distortion values. Eq. 5.15 is a linear observation equation. For every distortion value, an observation equation is obtained.

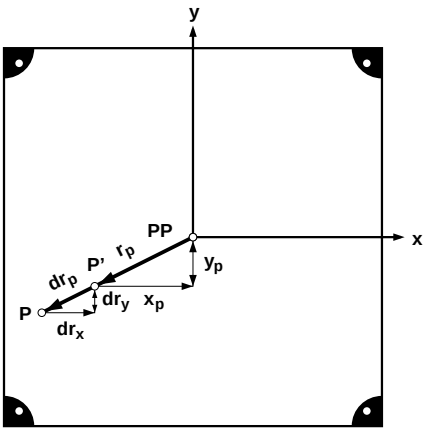

Figure 5.4: Correction for radial distortion.

In order to avoid numerical problems (ill-conditioned normal equation system), the degree of the polynom should not exceed nine.

5.3.4 Correction for Refraction

Fig. 5.5 shows how an oblique light ray is refracted by the atmosphere. According to Snell's law, a light ray is refracted at the interface of two different media. The density differences in the atmosphere are in fact different media. The refraction causes the image to be displayed outwardly, quite similar to a positive radial distortion.

The radial displacement caused by refraction can be computed by

$$dref = K(r + \frac{r^3}{c^2}) \tag{5.16}$$

$$K = \left(\frac{2410\, H}{H^2 - 6\, H + 250} - \frac{2410\, h^2}{(h^2 - 6\, h + 250)H} \right) 10^{-6} \tag{5.17}$$

These equations are based on a model atmosphere defined by the US Air Force. The flying height H and the ground elevation h must be in units of kilometers.

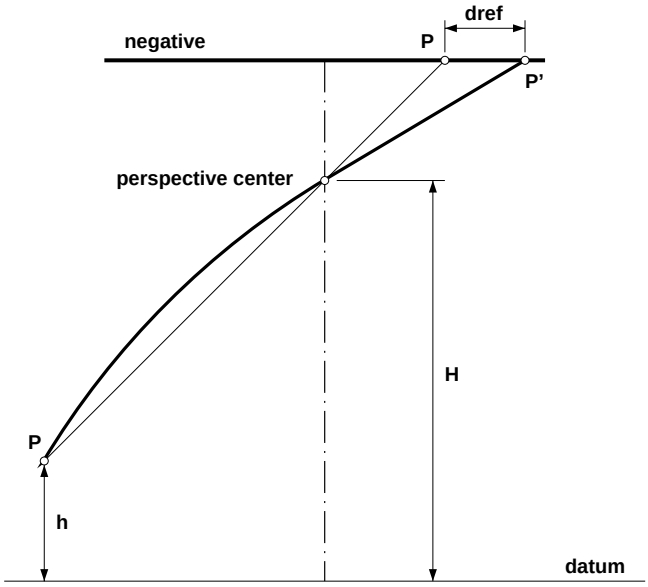

Figure 5.5: Correction for refraction.

5.3.5 Correction for Earth Curvature

As mentioned in the beginning of this Chapter, the mathematical derivation of the relationships between image and object space are based on the assumption that for both spaces, 3-D cartesian coordinate systems are employed. Since ground control points may not directly be available in such a system, they must first be transformed, say from a State Plane coordinate system to a cartesian system.

The X and Y coordinates of a State Plane system are cartesian, but not the elevations. Fig. 5.6 shows the relationship between elevations above a datum and elevations in the 3-D cartesian system. If we approximate the datum by a sphere, radius $R = 6372.2$ km, then the radial displacement can be computed by

$$dearth = \frac{r^3\,(H - Z_P)}{2\,c^2\,R} \tag{5.18}$$

Like radial distortion and refraction, the corrections in $x-$ and y-direction is readily determined by Eq. 4.13 and 5.14. Strictly speaking, the correction of photo-coordinates due to earth curvature is not a refinement of the mathematical model. It is much better to eliminate the influence of earth curvature by transforming the object space into a 3-D cartesian system before establishing relationships with the ground system. This is always possible, except when compiling a map. A map, generated on an analytical plotter, for example, is most likely plotted in a State Plane coordinate system. That is,

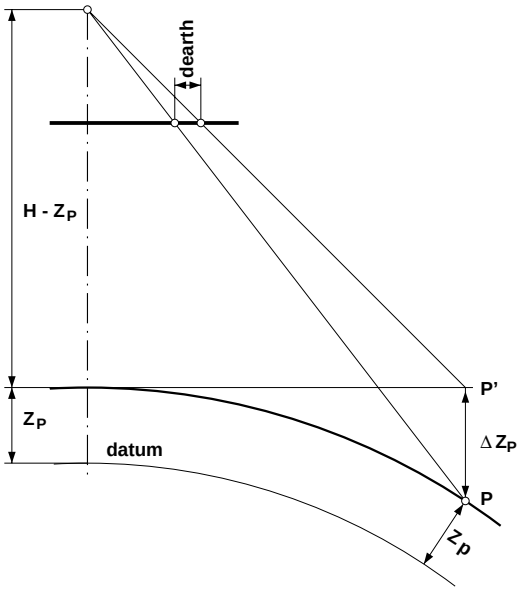

Figure 5.6: Correction of photo-coordinates due to earth curvature.

the elevations refer to the datum and not to the XY plane of the cartesian coordinate system. It would be quite awkward to produce the map in the cartesian system and then transform it to the target system. Therefore, during map compilation, the photo-coordinates are “corrected" so that conjugate bundle rays intersect in object space at positions related to reference sphere.

5.3.6 Summary of Computing Photo-Coordinates

We summarize the main steps necessary to determine photo-coordinates. The process to correct them for systematic errors, such as radial distortion, refraction and earth curvature is also known as *image refinement*. Fig. 5.7 depicts the coordinate systems involved, an imaged point P, and the correction vectors *dr, dref, dearth*.

1. Insert the diapositive into the measuring system (e.g. comparator, analytical plotter) and measure the fiducial marks in the machine coordinate system *xm, ym*. Compute the transformation parameters with a similarity or affine transformation. The transformation establishes a relationship between the measuring system and the fiducial coordinate system.

2. Translate the fiducial system to the photo-coordinate system (Eqs. 4.6 and 5.7).

3. Correct photo-coordinates for radial distortion. The radial distortion dr_p for point

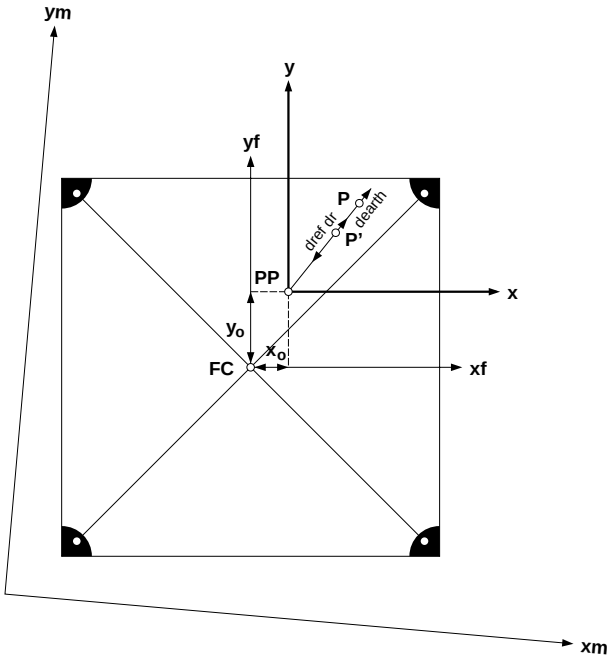

Figure 5.7: Interior orientation and image refinement.

P is found by linearly interpolating the values given in the calibration protocol (Eq. 5.10).

4. Correct the photo-coordinates for refraction, according to Eqs. 4.16 and 5.17. This correction is negative. The displacement caused by refraction is a functional relationship of *dref* $= f(H, h, r, c)$. With a flying height $H = 2,000\ m$, elevation above ground $h = 500\ m$ we obtain for a wide angle camera ($c \approx 0.15\ m$) a correction of $-4\,\mu m$ for $r = 130$ mm. An extreme example is a superwide angle camera, $H = 9,000$ m, $h = 500$ m, where *dref* $= -34\ \mu m$ for the same point.

5. Correct for earth curvature only if the control points (elevations) are not in a cartesian coordinate system or if a map is compiled. Using the extreme example as above, we obtain *dearth* $= 65\ \mu$m. Since this correction has the opposite sign of the refraction, the combined correction for refraction and earth curvature would be *dcomb* $= 31\ \mu m$. The correction due to earth curvature is larger than the correction for refraction.

5.4 Exterior Orientation

Exterior orientation is the relationship between image and object space. This is accomplished by determining the camera position in the object coordinate system. The camera position is determined by the location of its perspective center and by its attitude, expressed by three independent angles.

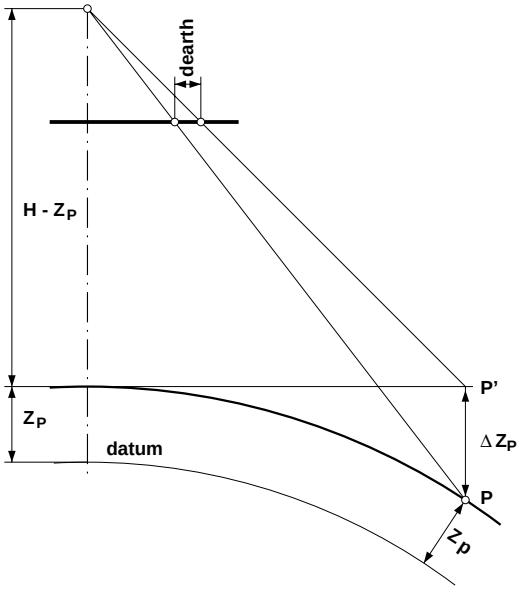

Figure 5.8: Exterior Orientation.

The problem of establishing the six orientation parameters of the camera can conveniently be solved by the collinearity model. This model expresses the condition that the perspective center C, the image point P_i, and the object point P_o, must lie on a straight line (see Fig. 5.8). If the exterior orientation is known, then the image vector $\mathbf{p}_i$ and the vector $\mathbf{q}$ in object space are collinear:

$$\mathbf{p}_i = \frac{1}{\lambda}\mathbf{q} \tag{5.19}$$

As depicted in Fig. 5.8, vector $\mathbf{q}$ is the difference between the two point vectors $\mathbf{c}$ and $\mathbf{p}$. For satisfying the collinearity condition, we rotate and scale $\mathbf{q}$ from object to image space. We have

$$\mathbf{p}_i = \frac{1}{\lambda}\mathbf{R}\,\mathbf{q} = \frac{1}{\lambda}\mathbf{R}\,(\mathbf{p} - \mathbf{c}) \tag{5.20}$$

with $\mathbf{R}$ an orthogonal rotation matrix with the three angles ω, ϕ and κ:

$$\mathbf{R} = \begin{vmatrix} \cos\phi\cos\kappa & -\cos\phi\sin\kappa & \sin\phi \\ \cos\omega\sin\kappa + \sin\omega\sin\phi\cos\kappa & \cos\omega\cos\kappa - \sin\omega\sin\phi\sin\kappa & -\sin\omega\cos\phi \\ \sin\omega\sin\kappa - \cos\omega\sin\phi\cos\kappa & \sin\omega\cos\kappa + \cos\omega\sin\phi\sin\kappa & \cos\omega\cos\phi \end{vmatrix} \tag{5.21}$$

Eq. 5.20 renders the following three coordinate equations.

$$x = \frac{1}{\lambda}(X_P - X_C)r_{11} + (Y_P - Y_C)r_{12} + (Z_P - Z_C)r_{13} \tag{5.22}$$

$$y = \frac{1}{\lambda}(X_P - X_C)r_{21} + (Y_P - Y_C)r_{22} + (Z_P - Z_C)r_{23} \tag{5.23}$$

$$-c = \frac{1}{\lambda}(X_P - X_C)r_{31} + (Y_P - Y_C)r_{32} + (Z_P - Z_C)r_{33} \tag{5.24}$$

By dividing the first by the third and the second by the third equation, the scale factor $\frac{1}{\lambda}$ is eliminated leading to the following two collinearity equations:

$$x = -c\frac{(X_P - X_C)r_{11} + (Y_P - Y_C)r_{12} + (Z_P - Z_C)r_{13}}{(X_P - X_C)r_{31} + (Y_P - Y_C)r_{32} + (Z_P - Z_C)r_{33}} \tag{5.25}$$

$$y = -c\frac{(X_P - X_C)r_{21} + (Y_P - Y_C)r_{22} + (Z_P - Z_C)r_{23}}{(X_P - X_C)r_{31} + (Y_P - Y_C)r_{32} + (Z_P - Z_C)r_{33}} \tag{5.26}$$

with:

$$\mathbf{p}_i = \begin{bmatrix} x \\ y \\ -f \end{bmatrix} \qquad \mathbf{p} = \begin{bmatrix} X_P \\ Y_P \\ Z_P \end{bmatrix} \qquad \mathbf{c} = \begin{bmatrix} X_C \\ Y_C \\ Z_C \end{bmatrix}$$

The six parameters: $X_C, Y_C, Z_C, \omega, \phi, \kappa$ are the unknown elements of exterior orientation. The image coordinates x, y are normally known (measured) and the calibrated focal length c is a constant. Every measured point leads to two equations, but also adds three other unknowns, namely the coordinates of the object point (X_P, Y_P, Z_P). Unless the object points are known (control points), the problem cannot be solved with only one photograph.

The collinearity model as presented here can be expanded to include parameters of the interior orientation. The number of unknowns will be increased by three[2]. This combined approach lets us determine simultaneously the parameters of interior and exterior orientation of the cameras.

There are only limited applications for single photographs. We briefly discuss the computation of the exterior orientation parameters, also known as single photograph resection, and the computation of photo-coordinates with known orientation parameters. Single photographs cannot be used for the main task of photogrammetry, the reconstruction of object space. Suppose we know the exterior orientation of a photograph. Points in object space are not defined, unless we also know the scale factor $1/\lambda$ for every bundle ray.

[2]Parameters of interior orientation: position of principal point and calibrated focal length. Additionally, three parameters for radial distortion and three parameters for tangential distortion can be added.

5.4.1 Single Photo Resection

The position and attitude of the camera with respect to the object coordinate system (exterior orientation of camera) can be determined with help of the collinearity equations. Eqs. 5.26 and 4.27 express measured quantities[3] as a function of the exterior orientation parameters. Thus, the collinearity equations can be directly used as observation equations, as the following functional representation illustrates.

$$x, y = f(\underbrace{X_C, Y_C, Z_C, \omega, \phi, \kappa}_{\text{exterior orientation}}, \underbrace{X_P, Y_P, Z_P}_{\text{object point}}) \tag{5.27}$$

For every measured point two equations are obtained. If three control points are measured, a total of 6 equations is formed to solve for the 6 parameters of exterior orientation.

The collinearity equations are not linear in the parameters. Therefore, Eqs. 4.25 and 5.26 must be linearized with respect to the parameters. This also requires approximate values with which the iterative process will start.

5.4.2 Computing Photo Coordinates

With known exterior orientation elements photo-coordinates can be easily computed from Eqs. 4.25 and 5.26. This is useful for simulation studies where synthetic photo-coordinates are computed.

Another application for the direct use of the collinearity equations is the real-time loop of analytical plotters where photo-coordinates of ground points or model points are computed after relative or absolute orientation (see next chapter, analytical plotters).

5.5 Orientation of a Stereopair

5.5.1 Model Space, Model Coordinate System

The application of single photographs in photogrammetry is limited because they cannot be used for reconstructing the object space. Even though the exterior orientation elements may be known it will not be possible to determine ground points unless the scale factor of every bundle ray is known. This problem is solved by exploiting stereopsis, that is by using a second photograph of the same scene, taken from a different position.

Two photographs with different camera positions that show the same area, at least in part, is called a *stereopair*. Suppose the two photographs are oriented such that *conjugate points* (corresponding points) intersect. We call this intersection space *model space*. In order for expressing relationships of this model space we introduce a reference system, the *model coordinate system*. This system is 3-D and cartesian. Fig. 5.9 illustrates the concept of model space and model coordinate system.

Introducing the model coordinate system requires the definition of its spatial position (origin, attitude), and its scale. These are the seven parameters we have encountered

[3] We assume that the photo-coordinates are measured. In fact they are derived from measured machine coordinates. The correlation caused by the transformation is neglected.

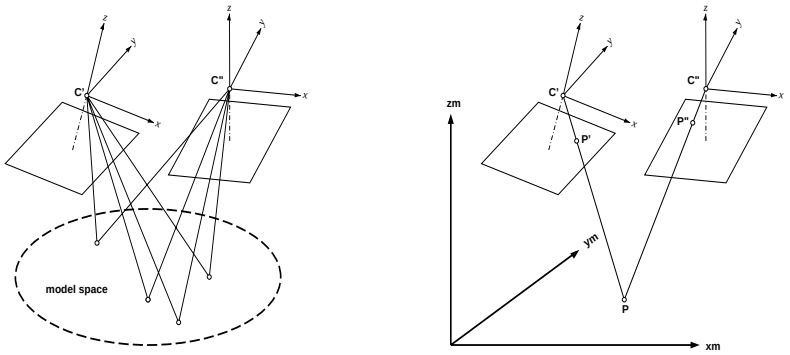

Figure 5.9: The concept of model space (a) and model coordinate system (b).

in the transformation of 3-D cartesian systems. The decision on how to introduce the parameters depends on the application; one definition of the model coordinate system may be more suitable for a specific purpose than another. In the following subsections, different definitions will be discussed.

Now the orientation of a stereopair amounts to determining the exterior orientation parameters of both photographs, with respect to the model coordinate system. From single photo resection, we recall that the collinearity equations form a suitable mathematical model to express the exterior orientation. We have the following functional relationship between observed photo-coordinates and orientation parameters:

$$x, y = f(\underbrace{X'_C, Y'_C, Z'_C, \omega', \phi', \kappa'}_{\text{ext. or}'}, \underbrace{X''_C, Y''_C, Z''_C, \omega'', \phi'', \kappa''}_{\text{ext. or}''}, \underbrace{X_1, Y_1, Z_1}_{\text{mod. pt 1}}, \cdots, \underbrace{X_n, Y_n, Z_n)}_{\text{mod. pt n}} \quad (5.28)$$

where f refers to Eqs. 4.25 and 5.26. Every point measured in one photo-coordinate system renders two equations. The same point must also be measured in the second photo-coordinate system. Thus, for one model point we obtain 4 equations, or $4\,n$ equations for n object points. On the other hand, n unknown model points lead to $3\,n$ parameters, or to a total $12 + 3\,n - 7$. These are the exterior orientation elements of both photographs, minus the parameters we have eliminated by defining the model coordinate system. By equating the number of equations with number of parameters we obtain the minimum number of points, n_{min}, which we need to measure for solving the orientation problem.

$$4\,n_{\text{min}} = 12 - 7 + 3\,n_{\text{min}} \qquad \Longrightarrow \qquad n_{\text{min}} = 5 \quad (5.29)$$

The collinearity equations which are implicitly referred to in Eq. 5.28 are non-linear. By linearizing the functional form we obtain

$$x, y \approx f^0 + \frac{\vartheta f}{\vartheta X'_C}\Delta X'_C + \frac{\vartheta f}{\vartheta Y'_C}\Delta Y'_C + \cdots + \frac{\vartheta f}{\vartheta Z''_C}\Delta Z''_C \quad (5.30)$$

with f^0 denoting the function with initial estimates for the parameters.

For a point P_i, $i = 1, \cdots, n$ we obtain the following four generic observation equations

$$\begin{aligned}
r'_{xi} &= \frac{\vartheta f}{\vartheta X'_C}\Delta X'_C + \frac{\vartheta f}{\vartheta Y'_C}\Delta Y'_C + \cdots + \frac{\vartheta f}{\vartheta Z''_C}\Delta Z''_C + f^0 - x'_i \\
r'_{yi} &= \frac{\vartheta f}{\vartheta X'_C}\Delta X'_C + \frac{\vartheta f}{\vartheta Y'_C}\Delta Y'_C + \cdots + \frac{\vartheta f}{\vartheta Z''_C}\Delta Z''_C + f^0 - y'_i \\
r''_{xi} &= \frac{\vartheta f}{\vartheta X'_C}\Delta X'_C + \frac{\vartheta f}{\vartheta Y'_C}\Delta Y'_C + \cdots + \frac{\vartheta f}{\vartheta Z''_C}\Delta Z''_C + f^0 - x''_i \\
r''_{yi} &= \frac{\vartheta f}{\vartheta X'_C}\Delta X'_C + \frac{\vartheta f}{\vartheta Y'_C}\Delta Y'_C + \cdots + \frac{\vartheta f}{\vartheta Z''_C}\Delta Z''_C + f^0 - y''_i
\end{aligned} \tag{5.31}$$

As mentioned earlier, the definition of the model coordinate system reduces the number of parameters by seven. Several techniques exist to consider this in the least squares approach.

1. The simplest approach is to eliminate the parameters from the parameter list. We will use this approach for discussing the dependent and independent relative orientation.

2. The knowledge about the 7 parameters can be introduced in the mathematical model as seven independent pseudo observations (e.g. $\Delta X_C = 0$), or as condition equations which are added to the normal equations. This second technique is more flexible and it is particularly suited for computer implementation.

5.5.2 Dependent Relative Orientation

The definition of the model coordinate system in the case of a dependent relative orientation is depicted in Fig. 5.10. The position and the orientation is identical to one of the two photo-coordinate systems, say the primed system. This step amounts to introducing the exterior orientation of the photo-coordinate system as known. That is, we can eliminate it from the parameter list. Next, we define the scale of the model coordinate system. This is accomplished by defining the distance between the two perspective centers (base), or more precisely, by defining the X-component.

With this definition of the model coordinate system we are left with the following functional model

$$x, y = f(\underbrace{ym''_c, zm''_c, \omega'', \phi'', \kappa''}_{\text{ext. or}''}, \underbrace{xm_1, ym_1, zm_1}_{\text{model pt 1}}, \cdots, \underbrace{xm_n, ym_n, zm_n}_{\text{model pt n}}) \tag{5.32}$$

With 5 points we obtain 20 observation equations. On the other hand, there are 5 exterior orientation parameters and 5×3 model coordinates. Usually more than 5 points are measured. The redundancy is $r = n - 5$. The typical case of relative orientation

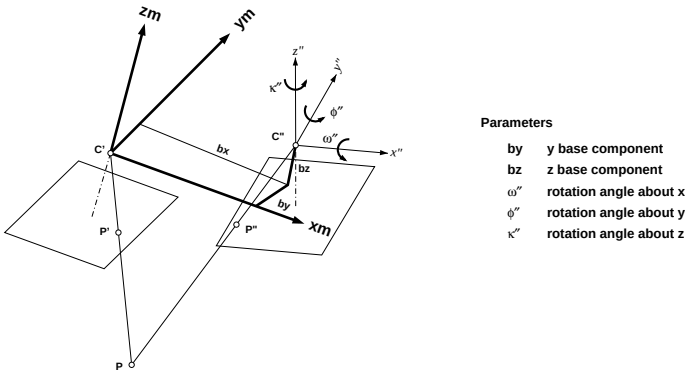

Figure 5.10: Definition of the model coordinate system and orientation parameters in the dependent relative orientation.

on a stereoplotter with the 6 von Gruber points leads only to a redundancy of one. It is highly recommended to measure more, say 12 points, in which case we find $r = 7$.

With a non linear mathematical model we need be concerned with suitable approximations to ensure that the iterative least squares solution converges. In the case of the dependent relative orientation we have

$$f^0 = f(yc_c^0, zm_c^0, \omega^0, \phi^0, \kappa^0, xm_1^0, ym_1^0, zm_1^0, \cdots, xm_n^0, ym_n^0, zm_n^0) \tag{5.33}$$

The initial estimates for the five exterior orientation parameters are set to zero for aerial applications, because the orientation angles are smaller than five degrees, and $xm_c >> ym_c,\ xm_c >> zm_c \implies ym_c^0 = zm_c^0 = 0$. Initial positions for the model points can be estimated from the corresponding measured photo-coordinates. If the scale of the model coordinate system approximates the scale of the photo-coordinate system, we estimate initial model points by

$$\begin{aligned} xm_i^0 &\approx x_i' \\ ym_i^0 &\approx y_i' \\ zm_i^0 &\approx z_i' \end{aligned} \tag{5.34}$$

The dependent relative orientation leaves one of the photographs unchanged; the other one is oriented with respect to the unchanged system. This is of advantage for the conjunction of successive photographs in a strip. In this fashion, all photographs of a strip can be joined into the coordinate system of the first photograph.

5.5.3 Independent Relative Orientation

Fig. 5.11 illustrates the definition of the model coordinate system in the independent relative orientation.

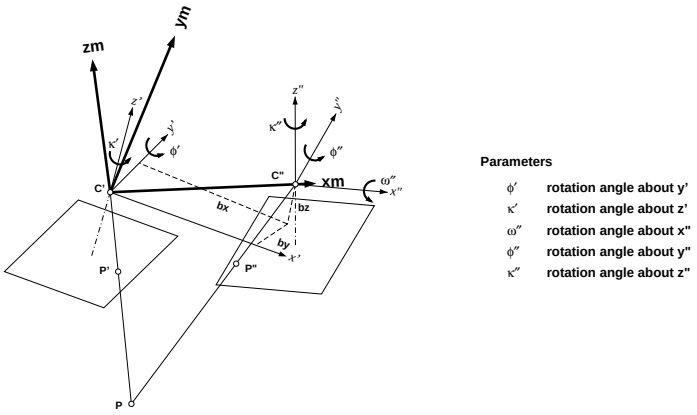

Figure 5.11: Definition of the model coordinate system and orientation parameters in the independent relative orientation.

The origin is identical to one of the photo-coordinate systems, e.g. in Fig. 5.11 it is the primed system. The orientation is chosen such that the positive xm-axis passes through the perspective center of the other photo-coordinate system. This requires determining two rotation angles in the primed photo-coordinate system. Moreover, it eliminates the base components *by, bz*. The rotation about the x-axis (ω) is set to zero. This means that the ym-axis is in the $x - y$ plane of the photo-coordinate system. The scale is chosen by defining $xm''_c = bx$.

With this definition of the model coordinate system we have eliminated the position of both perspective centers and one rotation angle. The following functional model applies

$$x, y = f(\underbrace{\phi', \kappa'}_{\text{ext.or.}'} , \underbrace{\omega'', \phi'', \kappa''}_{\text{ext.or.}''} , \underbrace{xm_1, ym_1, zm_1}_{\text{model pt 1}}, \cdots , \underbrace{xm_n, ym_n, zm_n)}_{\text{model pt n}} \qquad (5.35)$$

The number of equations, number of parameters and the redundancy are the same as in the dependent relative orientation. Also, the same considerations regarding initial estimates of parameters apply.

Note that the exterior orientation parameters of both types of relative orientation are related. For example, the rotation angles ϕ', κ' can be computed from the spatial direction of the base in the dependent relative orientation.

$$\phi' = \arctan(\frac{zm_c''}{bx}) \tag{5.36}$$

$$\kappa' = \arctan(\frac{ym_c''}{(bx^2 + zm_c^2)^{1/2}}) \tag{5.37}$$

5.5.4 Direct Orientation

In the direct orientation, the model coordinate system becomes identical with the ground system, for example, a State Plane coordinate system (see Fig. 5.12). Since such systems are already defined, we cannot introduce a priori information about exterior orientation parameters like in both cases of relative orientation. Instead we use information about some of the object points. Points with known coordinates are called *control points*. A point with all three coordinates known is called *full control point*. If only X and Y is known then we have a *planimetric control point*. Obviously, with an *elevation control point* we know only the Z coordinate.

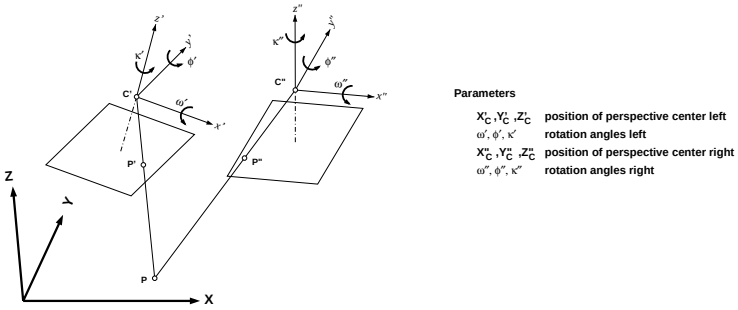

Figure 5.12: Direct orientation of a stereopair with respect to a ground control coordinate system.

The required information about 7 independent coordinates may come from different arrangements of control points. For example, 2 full control points and an elevation, or two planimetric control points and three elevations, will render the necessary information. The functional model describing the latter case is given below:

$$x, y = f(\underbrace{X_C', Y_C', Z_C', \omega', \phi', \kappa'}_{\text{ext. or}'}, \underbrace{X_C'', Y_C'', Z_C'', \omega'', \phi'', \kappa''}_{\text{ext. or}''}, \underbrace{Z_1, Z_2, X_3, Y_3, X_4, Y_4, X_5, Y_5}_{\text{unknown coord. of ctr. pts}}) \tag{5.38}$$

The Z-coordinates of the planimetric control points 1 and 2 are not known and thus remain in the parameter list. Likewise, $X - Y$-coordinates of elevation control points $3, 4, 5$ are parameters to be determined. Let us check the number of observation equations for this particular case. Since we measure the five partial control points on both

photographs we obtain 20 observation equations. The number of parameters amounts to 12 exterior orientation elements and 8 coordinates. So we have just enough equations to solve the problem. For every additional point 4 more equations and 3 parameters are added. Thus, the redundancy increases linearly with the number of points measured. Additional control points increase the redundancy more, e.g. full control points by 4, an elevation by 2.

Like in the case of relative orientation, the mathematical model of the direct orientation is also based on the collinearity equations. Since it is non-linear in the parameters we need good approximations to assure convergence. The estimation of initial values for the exterior orientation parameters may be accomplished in different ways. To estimate X_C^0, Y_C^0 for example, one could perform a 2-D transformation of the photo coordinates to planimetric control points. This would also result in a good estimation of κ^0 and of the photo scale which in turn can be used to estimate $Z_C^0 = \text{scale}\, c$. For aerial applications we set $\omega^0 = \phi^0 = 0$. With these initial values of the exterior orientation one can compute approximations X_i^0, Y_i^0 of object points where $Z_i^0 = h_{\text{aver}}$.

Note that the minimum number of points to be measured in the relative orientation is 5. With the direct orientation, we need only three points assuming that two are full control points. For orienting stereopairs with respect to a ground system, there is no need to first perform a relative orientation followed by an absolute orientation. This traditional approach stems from analog instruments where it is not possible to perform a direct orientation by mechanical means.

5.5.5 Absolute Orientation

With absolute orientation we refer to the process of orienting a stereomodel to the ground control system. Fig. 5.13 illustrates the concept. This is actually a very straightforward task which we discussed earlier under 7-parameter transformation. Note that the 7-parameter transformation establishes the relationship between two 3-D Cartesian coordinate systems. The model coordinate system is cartesian, but the ground control system is usually not cartesian because the elevations refer to a separate datum. In that case, the ground control system must first be transformed into an orthogonal system.

The transformation can only be solved if a priori information about some of the parameters is introduced. This is most likely done by control points. The same considerations apply as just discussed for the direct orientation.

From Fig. 5.13 we read the following vector equation which relates the model to the ground control coordinate system:

$$\mathbf{p} = s\mathbf{R}\mathbf{pm} - \mathbf{t} \tag{5.39}$$

where $\mathbf{pm} = [xm, ym, zm]^T$ is the point vector in the model coordinate system, $\mathbf{p} = [X, Y, Z]^T$ the vector in the ground control system pointing to the object point P and $\mathbf{t} = [X_t, Y_t, Z_t]^T$ the translation vector between the origins of the 2 coordinate systems. The rotation matrix $\mathbf{R}$ rotates vector $\mathbf{pm}$ into the ground control system and s, the scale factor, scales it accordingly. The 7 parameters to be determined comprise 3 rotation angles of the orthogonal rotation matrix $\mathbf{R}$, 3 translation parameters and one scale factor.

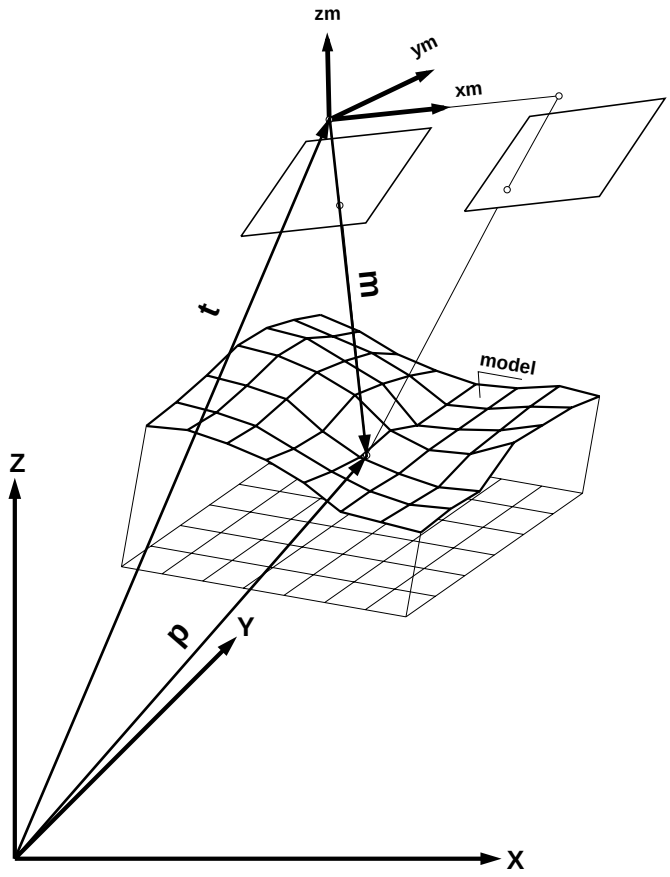

Figure 5.13: Absolute orientation entails the computation of the transformation parameters between model and ground coordinate system.

The following functional model applies:

$$x, y, z = f(\underbrace{X_t, Y_t, Z_t}_{\text{translation}}, \underbrace{\omega, \phi, \kappa}_{\text{orientation}}, \underbrace{s}_{\text{scale}}) \tag{5.40}$$

In order to solve for the 7 parameters at least seven equations must be available. For example, 2 full control points and one elevation control point would render a solution. If more equations (that is, more control points) are available then the problem of determining the parameters can be cast as a least-squares adjustment. Here, the idea is to minimize the discrepancies between the transformed and the available control points. An observation equation for control point P_i in vector form can be written as

$$\mathbf{r_i} = s\mathbf{R}\mathbf{p}\mathbf{m_i} - \mathbf{t} - \mathbf{p_i} \tag{5.41}$$

with $\mathbf{r}$ the residual vector $[r_x, r_y, r_z]^T$. Obviously, the model is not linear in the parameters. As usual, linearized observation equations are obtained by taking the partial derivatives with respect to the parameters. The linearized component equations are

The approximations may be obtained by first performing a 2-D transformation with x, y-coordinates only.

Chapter 6

Measuring Systems

Most analytical photogrammetric procedures require photo coordinates as measured quantities. This, in turn, requires accurate, reliable and efficient devices for measuring points on stereo images. The accuracy depends on the application. Typical accuracies range between three and ten micrometers. Consequently, the measuring devices must meet an absolute, repeatable accuracy of a few micrometers over the entire range of the photographs, that is over an area of 230 mm $\times$ 230 mm.

In this chapter we discuss the basic functionality and working principles of analytical plotters and digital photogrammetric workstations.

6.1 Analytical Plotters

6.1.1 Background

The analytical plotter was invented in 1957 by Helava. The innovative concept was met with reservation because computers at that time were not readily available, expensive, and not very reliable. It took nearly 20 years before the major manufacturers of photogrammetric equipment embarked on the idea and began to develop analytical plotters. At the occasion of the ISPRS congress in 1976, analytical plotters were displayed for the first time to photogrammetrists from all over the world. Fig.6.1 shows a typical analytical plotter.

Slowly, analytical plotters were bought to replace analog stereoplotters. By 1980, approximately 5,500 stereoplotters were in use worldwide, but only a few hundred analytical plotters. Today, this number increased to approximately 1,500. Leica and Zeiss are the main manufacturers with a variety of systems. However, production of instruments has stopped in the early 1990s.

6.1.2 System Overview

Fig. 6.2 depicts the basic components of an analytical plotter. These components comprise the stereo viewer, the user interface, electronics and real-time processor, and host computer.

Figure 6.1: SD2000 analytical plotter from Leica.

Stereo Viewer

The viewing system resembles closely a stereo comparator, particularly the binocular system with high quality optics, zoom lenses, and image rotation. Also, the measuring mark and the illumination system are refined versions of stereocomparator components. Fig 6.3 shows a typical viewer with the binocular system, the stages, and the knobs for adjusting the magnification, illumination and image rotation.

The size of the stages must allow for measuring aerial photographs. Some instruments offer larger stage sizes, for example 18×9 in. to accomodate panoramic imagery.

An important part of the stereo viewer is the measuring and recording system. As discussed in the previous section, the translation of the stages, the measuring and recording is all combined by employing either linear encoders or spindles.

Translation System

In order to move the measuring mark from one point to another either the viewing system must move with respect to a stationary measuring system, or the measuring system, including photograph, moves against a fixed viewing system. Most x-y-comparators have a moving stage system. The carrier plate on which the diapositive is clamped, moves against a pair of fixed glass scales and the fixed viewing system (compare also Fig. 6.5).

In most cases, the linear translation is accomplished by purely mechanical means. Fig. 6.4 depicts some typical translation guides. Various forms of bearings are used to

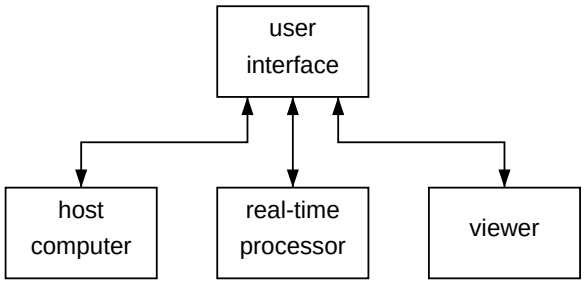

Figure 6.2: The main components of an analytical plotter.

Figure 6.3: Stereo viewer of the Planicomp P-3 analytical plotter from Zeiss.

reduce friction and wear and tear. An interesting solution are air bearings. The air is pumped through small orifices located on the facing side of one of two flat surfaces. This results in a thin uniform layer of air separating the two surfaces, providing smooth motion.

The force to produce motion is most often produced by threaded spindles or precision lead screws. Coarse positioning is most conveniently accomplished by a free moving cursor. After clamping the stages, a pair of handwheels allows for precise positioning.

Measuring and Recording System

If the translation system uses precision lead screws then the measuring is readily accomplished by counting the number of rotations of the screw. For example, a single rotation would produce a relative translation equal to the pitch of the screw. If the pitch is uniform, a fractional part of the rotation can be related to a fractional part of the

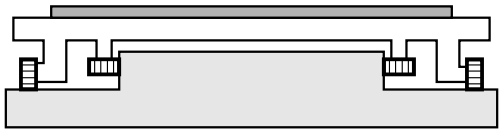

Figure 6.4: End view of typical translation way.

pitch. Full revolutions are counted on a coarse scale while the fractional part is usually interpreted on a separate, more accurate scale.

To record the measurements automatically, an analog to digital (A/D) conversion is necessary because the x-y-readings are analog in nature. Today, A/D converters are based on solid state electronics. They are very reliable, accurate and inexpensive.

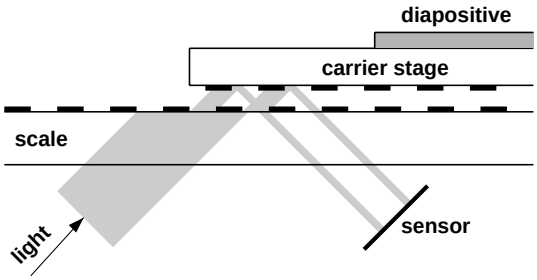

Figure 6.5: Working principle of linear encoders.

Fig. 6.5 illustrates one of several concepts for the A/D conversion process, using linear encoders. The grating of the glass scales is 40 μm. Light from the source L transmits through the glass scale and is reflected at the lower surface of the plate carrier. A photo diode senses the reflected light by converting it into a current that can be measured. Depending on the relative position of plate carrier and scale, more or less light is reflected. As can be seen from Fig. 6.5 there are two extreme positions where either no light or all light is reflected. Between these two extreme positions the amount of reflected light depends linearly on the movement of the plate carrier. Thus, the precise position is found by linear interpolation.

User Interface

With user interface we refer to the communication devices an operator has available to work on an analytical plotter. These devices can be associated to the following

functional groups:

viewer control buttons permit to change magnification, illumination and image rotation.

pointing devices are necessary to drive the measuring mark to specific locations,e.g. fiducial marks, control points or features to be digitized. Pointing devices include handwheels, footdisk, mouse, trackball, cursor. A typical configuration consists of a special cursor with an additional button to simulate z-movement (see Fig. 6.6). Handwheels and footdisk are usually offered as an option to provide the familiar environment of a stereoplotter.

digitizing devices are used to record the measuring mark together with addtional information such as identifiers, graphical attributes, feature codes. For obvious reasons, digitizing devices are usually in close proximity to pointing devices. For example, the cursor is often equipped with additional recording buttons. Digitizing devices may also come in the form of foot pedals, a typical solution found with stereoplotters. A popular digitizing device is the digitizing tablet that is mainly used to enter graphical information. Another solution is the function keyboard. It provides less flexibility, however.

host computer communication involves graphical user interface and keyboard.

Electronics and Real-Time Processor

The electronic cabinet and the real-time processor are the interface between the host computer and the stereo viewer. The user does not directly communicate with this sub-system.

The motors that drive the stages receive analog signals, for example voltage. However on the host computer only digital signals are available. Thus, the main function of the electronics is to accomplish A/D and D/A conversion.

Figure 6.6: Planicomp P-cursor as an example of a pointing and digitizing device.

The real-time processor is a natural consequence of the distributed computing concept. Its main task is to control the user interface and to perform the computing of

stage coordinates from model coordinates in real-time. This involves executing the collinearity equations and inverse interior orientation at a rate of 50 to 100 times per second.

Host Computer

The separation of real-time computations from more general computational tasks makes the analytical plotter a device independent peripheral with which the host communicates via standard interface and communication. The task of the host computer is to assist the operator in performing photogrammetric procedures such as the orientation of a stereomodel and its digitization.

The rapid performance increase of personal computers (PC) and their relatively low price makes them the natural choice for the host computer. Other hosts typically used are UNIX workstations.

Auxiliary Devices

Depending on the type of instruments, auxiliary devices may be optionally available to increase the functionality. On such device is the superpositioning system. Here, the current digitizing status is displayed on a small, high resolution monitor. The display is interjected into the optical path so that the operator sees the digitized map superimposed on the stereomodel.This is very helpful for quickly checking the completeness and the correctness of graphical information.

6.1.3 Basic Functionality

Analytical plotters work in two modes: stereocomparator mode and model mode. We first discuss the model mode because that is the standard operational mode.

Model Mode

Suppose we have set up a model. That is, the diapositives of a stereopair are placed on the stages and are oriented. The task is now to move the measuring mark to locations of interest, for example to features we need to digitize. How do the stages move to the conjugate location?

The measuring mark, together with the binoculars, remain fixed. As a consequence, the stages must move to go from one point to another. New positions are indicated by the pointing devices, for example by moving the cursor in the direction of the new point. The cursor position is constantly read by the real-time processor. The analog signal is converted to a 3-D location. One can think of moving the cursor in the 3-D model space. The 3-D model position is immediately converted to stage coordinates. This is accomplished by first computing photo-coordinates with the collinearity equations, followed by computing stage coordinates with the inverse interior orientation. We have symbolically

$$
\begin{array}{lcl}
X, Y, Z & = & \text{derived from movement of pointing device} \\
x', y' & = & f(\text{ext.or}', X, Y, Z, c')
\end{array}
$$

$$
\begin{array}{lcl}
x'', y'' & = & f(\text{ext.or}'', X, Y, Z, c'') \\
xm', ym' & = & f(\text{int.or}', x', y') \\
xm'', ym'' & = & f(\text{int.or}'', x'', y'')
\end{array}
$$

These equations symbolize the classical real-time loop of analytical plotters. The real-time processor is constantly reading the user interface. Changes in the pointing devices are converted to model coordinates X, Y, Z which, in turn, are transformed to stage coordinates xm, ym that are then submitted to the stage motors. This loop is repeated at least 50 times per second to provide smooth motion. It is important to realize that the pointing devices do not directly move the stages. Alternatively, model coordinates can also be provided by the host computer.

Comparator Mode

Clearly, the model mode requires the parameters of both, exterior and interior orientation. These parameters are only known after successful interior and relative orientation. Prior to this situation, the analytical plotter operates in the comparator mode. The same principle as explained above applies. The real-time processor still reads the position of the pointing devices. Instead of using the orientation parameters, approximations are used. For example, the 5 parameters of relative orientation are set to zero, and the same assumptions are made as discussed in Chapter 2, relative orientation. Since only rough estimates for the orientation parameters are used, conjugate locations are only approximate. The precise determination of conjugate points is obtained by clearing the parallaxes, exactly in the same way as with stereocomparators. Again, the pointing devices do not drive the stages directly.

6.1.4 Typical Workflow

In this section we describe a typical workflow, beginning with the definition of parameters, performing the orientations, and entering applications. Note that the communication is exclusively through the host computer, preferably by using a graphical user interface (GUI), such as Microsoft Windows.

Definition of System Parameters

After the installation of an analytical plotter certain system parameters must be defined. Some of these parameters are very much system dependent, particularly those related to the user interface. A good example is the sensitivity of pointing devices. One revolution of a handwheel corresponds to a linear movement in the model (actually to a translation of the stages). This value can be changed.

Other system parameters include the definition of units, such as angular units, or the definition of constants, such as earth radius. Some of the parameters are used as default values, that is, they can be changed when performing procedures involving them.

Definition of Auxiliary Data

Here we include information that is necessary to conduct the orientation procedures. For the interior orientation camera parameters are needed. This involves the calibrated focal lenght, the coordinates of the principal point, the coordinates of the fiducial marks, and the radial distortion. Different software varies in the degree of comfort and flexibility of entering data. For example, in most camera calibration protocols the coordinates of the fiducial marks are not explicitely available. They must be computed from distances measured between them. In that case, the host software should allow for entering distances, otherwise the user is required to compute coordinates.

For the absolute orientation control points are necessary. It is preferable to enter the control points prior to performing the absolute orientation. Also, it should be possible to import a ground control file if it already exists, say from computing surveying measurements. Camera data and control points should be independent from project data because several projects may use the same information.

Definition of Project Parameters

Project related information usually includes the project name and other descriptive data. At this level it is also convenient to define the number of parallax points, and the termination criteria for the orientation procedures, such as maximum number of iterations, or minimum changes of parameters between successive iterations.

More detailed information is required when defining the model parameters. The camera calibration data must be associated to the photography on the left and right stages. An option should exist to assign different camera names. Also, the ground control file name must be entered.

Interior Orientation

The interior orientation begins with placing the diapositives on the stages. Sometimes, the accessibility to the stages is limited, especially when they are parked at certain positions. In that case, the system should move the stages into a position of best accessibility. After having set all the necessary viewer control buttons, few parameters and options must be defined. This includes entering the camera file names and the choice of transformation to be used for the interior orientation. The system is now ready for measuring the fiducial marks. Based on the information in the camera file, approximate stage coordinates are computed for the stages to drive to. The fine positioning is performed with one of the pointing devices.

With every measurement improved positions of the next fiducial mark can be computed. For example, the first measurement allows to determine a better translation vector. After the second measurement, an improved value for the rotation angle is computed. In that fashion, the stages drive closer to the true position of every new fiducial mark. After the set of fiducial marks as specified in the calibration protocol is measured, the transformation parameters are computed and displayed, together with statistical results, such as residuals and standard deviation. Needless to say that throughout the interior orientation the system is in comparator mode.

Upon acceptance, the interior orientation parameters are downloaded to the real-time processor.

Relative Orientation

The relative orientation requires first a successful interior orientation. Prior to the measuring phase, certain parameters must be defined, for example the number of parallax points and the type of orientation (e.g. independent or dependent relative orientation). The analytical plotter is still in comparator mode. The stages are now directed to approximate locations of conjugate points, which are regularly distributed accross the model. The approximate positions are computed according to the consideration discussed in the previous section. Now, the operator selects a suitable point for clearing the parallaxes. This is accomplished by locking one stage and moving the other one only until a the point is parallax free.

After six points are measured, the parameters of relative orientation are computed and results are displayed. If the computation is successful, the parameters are downloaded to the RT processor and a model is established. At that time, the analytical plotter switches to the model mode. Now, the operator moves in an oriented model. To measure additional points, the system changes automatically to comparator mode to force the operator to clear the parallaxes.

It is good practice to include the control points in the measurements and computations of the relative orientation. Also, it is advisable to measure twelve or more points.

Absolute Orientation

The absolute orientation requires a successful interior and relative orientation. In case the control points are measured during the relative orientation, the system immediately computes the absolute orientation. As soon as the minimum control information is measured, the system computes approximate locations for additional control points and positions the stages accordingly.

6.1.5 Advantages of Analytical Plotters

The following table summarizes some of the advantages of analytical plotters over computer-assisted or standard stereoplotters. With computer-assisted plotters we mean a stereoplotter with encoders attached to the machine coordinate system so that model coordinates can be recorded automatically. A computer processes then the data and determines orientation parameters, for example. Those parameters must be turned in maually, however.

6.2 Digital Photogrammetric Workstations

Probably the single most significant product of digital photogrammetry is the *digital photogrammetric workstation (DPW)*, also called a *softcopy workstation*. The role of DPWs in digital photogrammetry is equivalent to that of analytical plotters in analytical photogrammetry.

Table 6.1: Comparison analytical plotters/stereoplottes.

Feature	*Analytical Plotter*	*Computer-assisted Stereoplotter*	*Conventional Stereoplotter*
accuracy			
instrument	2 μm	$\geq 10\mu$m	$\geq 10\mu$m
image refinement	yes	no	no
drive to			
FM, control points	yes	no	no
profiles	yes	yes	yes
DEM grid	yes	no	no
photography			
projection system	any	only central	only central
size	$\leq 18 \times 9$ in.	$\leq 9 \times 9$ in.	$\leq 9 \times 9$ in.
orientations			
computer assistance	high	medium	none
time	10 minutes	30 minutes	1 hour
storing parameters	yes	yes	no
range of or. parameters	unlimited	$\omega, \varphi \leq 5^o$	$\omega, \varphi \leq 5^o$
map compilation			
CAD systems	many	few	none
time	20 %	30 %	100 %

The development of DPWs is greatly influenced by computer technology. Considering the dynamic nature of this field, it is not surprising that digital photogrammetric workstations undergo constant changes, particularly in terms of performance, comfort level, components, costs, and vendors. It would be nearly impossible to provide a comprehensive list of the current products, which are commercially available much less describe them in some detail. Rather, the common aspects, such as architecture and functionality is emphasized.

The next section provides some background information, including a few historical remarks and an attempt to classify the systems. This is followed by a description of the basic system architecture and functionality. Finally, the most important applications are briefly discussed.

To build on common ground, I frequently compare the performance and functionality of DPWs with that of analytical plotters. Sec. 6.3 summarizes the advantages and the shortfalls of DPWs relative to analytical plotters.

6.2.1 Background

Great strides have been made in digital photogrammetry during the past few years due to the availability of new hardware and software, such as powerful image processing workstations and vastly increased storage capacity. Research and development efforts resulted in operational products that are increasingly being used by government organizations and private companies to solve practical photogrammetric problems. We are witnessing the transition from conventional to digital photogrammetry. DPWs play a key role in this transition.

Digital Photogrammetric Workstation and Digital Photogrammetry Environment

Fig. 6.7 depicts a schematic diagram of a digital photogrammetry environment. On the input side we have a digital camera or a scanner with which existing aerial photographs are digitized. At the heart of the processing side is the DPW. The output side may comprise a filmrecorder to produce hardcopies in raster format and a plotter for providing hardcopies in vector format. Some authors include the scanner and filmrecorder as components of the softcopy workstation. The view presented here is that a DPW is a separate, unique part of a digital photogrammetric system.

As discussed in the previous chapters, digital images are obtained directly by using electronic cameras, or indirectly by scanning existing photographs. The accuracy of digital photogrammetry products depends largely on the accuracy of electronic cameras or on scanners, and on the algorithms used. In contrast to analytical plotters (and even more so to analog stereoplotters), the hardware of DPWs has no noticeable effect on the accuracy.

Figs. 6.9 and 6.8 show typical digital photogrammetric workstations. At first sight they look much like ordinary graphics workstations. The major differences are the stereo display, 3-D measuring system, and increased storage capacity to hold all digital images of an entire project. Sec. 6.2.2 elaborates further on these aspects.

The station shown in Fig. 6.8 features two separate monitors. In this fashion, the stereo monitor is entirely dedicated to display imagery only. Additional information,

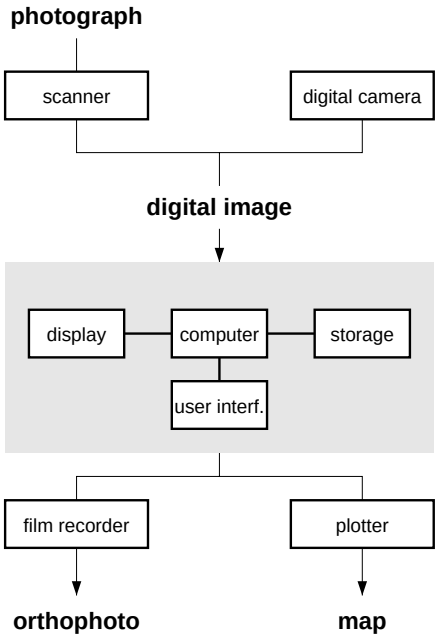

Figure 6.7: Schematic diagram of digital photogrammetry environment with the digital photogrammetric workstation (softcopy workstation) as the major component.

such as the graphical user interface, is displayed on the second monitor. As an option to the 3-D pointing device (trackball), the system can be equipped with handwheels to more closely simulate the operation on a classical instrument.

The main characteristic of Intergraph's ImageStation Z is the 28-inch panoramic monitor that provides a large field of view for stereo display (see Fig. 6.9, label 1). Liquid crystal glasses (label 3) ensure high-quality stereo viewing. The infrared emitter on top of the monitor (label 4) provides synchronization of the glasses and allows group viewing. The 3-D pointing device (label 6) allows freehand digitizing and the 10 buttons facilitate easy menu selection.

6.2.2 Basic System Components

Fig. 6.10 depicts the basic system components of a digital photogrammetric workstation.

CPU the central processing unit should be reasonably fast considering the amount of computations to be performed. Many processes lend themselves to parallel processing. Parallel processing machines are available at reasonable prices. However, programming that takes advantage of them is still a rare commodity and prevents a more wide spread use of the workstations.

Figure 6.8: Typical digital photogrammetric workstation. The system shown here offers optional handwheels to emulate operation on classical photogrammetric plotters. Courtesy LH Systems, Inc., San Diego, CA.

OS the operating system should be 32 bit based and suitable for real-time processing. UNIX satisfies these needs; in fact, UNIX based workstations were the systems of choice for DPWs until the emergence of Windows 95 and NT that make PCs a serious competitor of UNIX based workstations.

main memory due to the large amount of data to be processed, sufficient memory should be available. Typical DPW configurations have 64 MB, or more, of RAM.

storage system must accommodate the efficient storage of several images. It usually consists of a fast access storage device, e.g. hard disks, and mass storage media with slower access times. Sec. 6.2.3 discusses the storage system in more detail.

graphic system the graphics display system is another crucial component of the DPW. The purpose of the display processor is to fetch data, such as raster (images) or vector data (GIS), process and store it in the display memory and update the monitor. The display system also handles the mouse input and the cursor.

3-D viewing system is a distinct component of a DPWs usually not found in other workstations. It should allow viewing a photogrammetric model comfortably and possibly in color. For a human operator to see stereoscopically, the left and right image must be separated. Sec. 6.2.3 discusses the principles of stereo viewing.

3-D measuring device is used for stereo measurements by the operator. The solution may range from a combination of a 2-D mouse and trackball to an elaborate device with several programmable function buttons.

Figure 6.9: Digital photogrammetric workstation. Shown is Intergraph's ImageStation Z. Main characteristic is the large stereo display of the 28-inch panoramic monitor. Courtesy Intergraph Corporation, Huntsville, AL.

network a modern DPW hardly works in isolation. It is often connected to the scanning system and to other workstations, such as a geographic information system. The client/server concept provides an adequate solution in this scenario of multiple workstations and shared resources (e.g. printers, plotters).

user interface may consist of hardware components such as keyboard, mouse, and auxiliary devices like handwheels and footwheels (to emulate an analytical plotter environment). A crucial component is the graphical user interface (GUI).

6.2.3 Basic System Functionality

The basic system functionality can be divided into the following categories

1. *Archiving:* store and access images, including image compression and decompression.

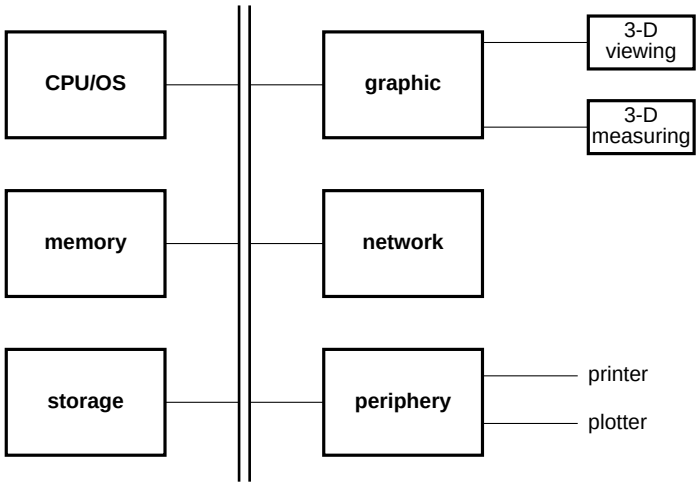

Figure 6.10: Basic system components of a digital photogrammetric workstation.

2. *Processing:* basic image processing tasks, such as enhancement and resampling.
3. *Display and Roam:* display images or sub-images, zoom in and out, roam within a model or an entire project.
4. *3-D Measurement:* interactively measure points and features to sub-pixel accuracy.
5. *Superpositioning:* measured data or existing digital maps must be superimposed on the displayed images.

A detailed discussion about the entire system functionality is beyond the scope of this book. We will focus on the storage system, on the display and measuring system, and on roaming.

Storage System

A medium size project in photogrammetric mapping contains hundreds of photographs. It is not uncommon to deal with thousands of photographs in large projects. Assuming digital images with 16 K $\times$ 16 K resolution (pixel size approx. 13 μm), a storage capacity of 256 MB per uncompressed black and white image is required. Consider a compression rate of three and we arrive at the typical number of 80 MB per image. To store a medium size project on-line causes heavy demands on storage.

Photogrammetry is not the only imaging application with high demands on storage, however. In medical imaging, for example, imaging libraries in the terabyte size are typical. Other examples of high storage demand applications include weather tracking and monitoring, compound document management, and interactive video. These

applications have a much higher market volume than photogrammetry; therefore, it is appealing for companies to further develop storage technologies.

The storage requirements in digital photogrammetry can be met through a carefully selected combination of available storage technologies. The options include:

hard disks: are an obvious choice, because of fast access and high performance capabilities. However, the high cost of disk space[1] would make it economically infeasible to store entire projects on disk drives. Therefore, hard disk drives are typically used for interactive and real-time applications, such as roaming or displaying spatially related images.

optical disks: have slower access times and lower data transfer rates but at lower cost (e.g. $10 to $15 per GB, depending on technology). The classical CD ROM and CD-R (writable) with a capacity of approximately 0.65 GB can hold only one stereomodel. A major effort is being devoted to increasing this capacity by an order of magnitude and make the medium a rewritable one. Until such systems become commercially available (including accepted standards), CDs are used mostly as a distribution media.

magnetic tape: offers the lowest media cost per GB (up to two orders of magnitude less than hard disk drives). Because of its slow performance (due to sequential access type), magnetic tapes are primarily used as backup devices. Recent advances in tape technology, however, make this device a viable option for on-line imaging application. Juke boxes with Exabyte or DLT (digital linear tape) cartridges (capacity of 20 to 40 GB per media) lend themselves into on-line image libraries with capacities of hundreds of gigabytes.

When designing a hierarchical storage system, factors such as storage capacity, access time, and transfer rates must be considered. Moreover, the way data is accessed, for example, randomly or sequentially, is important. Imagery requires inherently random access: think of roaming within a stereomodel. This seems to preclude the use of magnetic tapes for on-line applications. Clearly, one would not want to roam within a model stored on tape. However, if entire models are loaded from tape to hard disk, the access mode is not important, only the sustained transfer rate.

Viewing and Measuring System

An important aspect of any photogrammetric measuring system, be it analog or digital, is the viewing component. Viewing and measuring is typically performed stereoscopically, although certain operations do not require stereo capability.

As discussed in Chapter **??**, humans can discern 7 to 8 lp/mm at a normal viewing distance of 25 cm. To exploit the resolution of aerial films, say 70 lp/mm, it must be viewed under magnification. The oculars of analytical plotters have zoom optics that allow viewing the model at different magnifications[2]. Obviously, the larger the

[1] Every 18 months the storage capacity doubles, while the price per bit halves. As this book is written, hard disk drives sold for less than $100 per GB.

[2] Typical magnification values range from 5 to 20 times.

captionwidth7cm

Table 6.2: Magnification and size of field of view of analytical plotters.

magnification	*field of view, [mm]*		
	BC 1	*C120*	*P 1*
5 ×		29	40
6 ×	32		
10 ×		21	
15 ×		14	
20 ×	9	10	10

magnification the smaller the field of view. Table 6.2 lists zoom values and the size of the corresponding film area that appears in the oculars. Feature extraction (compilation) is usually performed with a magnification of 8 to 10 times. With higher magnification, the graininess of the film reduces the quality of stereoviewing. It is also worth pointing out that stereoscopic viewing requires a minimum field of view.

Let us now compare the viewing capabilities of analytical plotters with that of DPWs. First, we realize that this function is performed by the graphics subsystem, that is, by the monitor(s). To continue with the previous example of a film with 70 lp/mm resolution, viewed 10 × magnified, we read from Table 6.2 that the corresponding area on the film has a diameter of 20 mm. To preserve the high film resolution it ought to be digitized with a pixelsize of approximately 6 μm ($1000/(2 \times 70)$). It follows that the monitor should display more than $3K \times 3K$ pixels. Monitors with this sort of resolution do not exist or are prohibitively expensive, particularly when considering color imagery and true color rendition ($24+$ bit planes).

If we relax the high resolution requirements and assume that images are digitized with a pixelsize of 15 μm, then a monitor with the popular resolution of 1280 × 1024 would display an area that is quite comparable to that of analytical plotters.

Magnification, known under the more popular terms *zooming in/out*, is achieved by changing the ratio of number of image pixels displayed to the number of monitor pixels. To zoom in, more monitor pixels are used than image pixels. As a consequence, the size of the image viewed decreases and stereoscopic viewing may be affected.

The analogy to the floating point mark of analytical plotters is the three dimensional cursor that is created by using a pattern of pixels, such as a cross or a circle. The cursor must be generated by bitplane(s) that are not used for displaying the image. The cursor moves in increments of pixels, which may appear jerky compared to the smooth motion of analytical plotters. One advantage of cursors, however, is that they can be represented in any desirable shape and color.

The accuracy of interactive measurements depends on how well you can identify a feature, on the resolution, and on the cursor size. Ultimately, the pixelsize sets the lower limit. Assuming that the maximum error is 2 pixels, the standard deviation is approximately 0.5 pixel. A better sub-pixel accuracy can be obtained in two ways. A

straight-forward solution is to use more monitor pixels than image pixels. Fig. 6.11(a) exemplifies the situation. Suppose we use 3×3 monitor pixels to display one image pixel. The standard deviation of a measurement is now 0.15 image pixels[3]. As pointed out earlier, using more monitor pixels for displaying an image pixel reduces the size of the field of view. In the example above, only an area of 6 mm would be seen—hardly enough to support stereopsis.

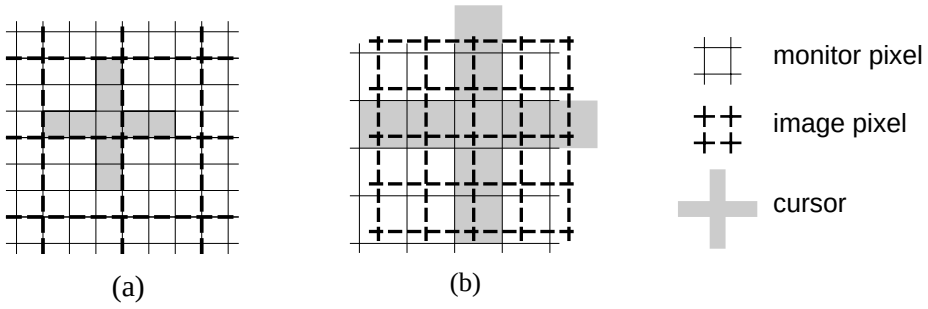

Figure 6.11: Two solutions to sub-pixel accuracy measurements. In (a), an image pixel is displayed to m monitor pixels, $m > 1$. The cursor moves in increments of monitor pixels, corresponding to $1/m$ image pixels. In (b) the image is moved under the fixed cursor position in increments smaller than an image pixel. This requires resampling the image at sub-pixel locations.

To circumvent the problem of reducing the field of view, an alternative approach to sub-pixel measuring accuracy is often preferred. Here, the cursor is fixed in the monitor's center and the image is moved instead. Now the image does not need to move in increments of pixels. Resampling at sub-pixel locations allows smaller movements. This solution requires resampling in real-time to assure smooth movement.

Yet another aspect is the illumination of the viewing system; so crucial when it comes to interpreting imagery. The brightness of the screen drops to 25% when polarization techniques are used[4]. Moreover, the phosphor latency causes ghost images. All these factors reduce the image quality.

In conclusion, we realize that viewing on a DPW is hampered in several ways and is far inferior to viewing the same scene on an analytical plotter. To alleviate the problems, high resolution monitors should be used.

Stereoscopic Viewing

An essential component of a DPW is the stereoscopic viewing system (even though a number of photogrammetric operations can be performed monoscopically). For a human operator to see stereoscopically, the left and right image must be separated.

[3] As before, the standard deviation is assumed to be 0.5 monitor pixel. We then obtain in the image domain an accuracy of $0.5 \times 1/3$ image pixel.

[4] Polarization absorbs half of the light. Another half is lost because the image is only viewed during half of the time usually available when viewing in monoscopic mode.

Table 6.3: Separation of images for stereoscopic viewing.

separation	*implementation*
spatial	2 monitors + stereoscope 1 monitor + stereoscope (split screen) 2 monitors + polarization
spectral	anaglyphic polarization
temporal	alternate display of left and right image synchronized by polarization

This separation is accomplished in different ways; for example, spatially, spectrally, or temporally (Table 6.3).

One may argue that the simplest way to achieve stereoscopic viewing is by displaying the two images of a stereopair on two separate monitors. Viewing is achieved by means of optical trains, e.g. a stereoscope, or by polarization. Matra adopted this principle by arranging the two monitors at right angles, with horizontal and vertical polarization sheets in front of them.

An example of the split-screen solution is shown in Fig. 6.12. Here, the left and right images are displayed on the left and right half of the monitor, respectively. A stereoscope, mounted in front of the monitor, provides viewing. Obviously, this solution permits only one person to view the model. A possible disadvantage is the resolution, because only half of the screen resolution[5] is available for displaying the model.

The most popular realization of spectral separation is by anaglyphs. The restriction to monochromatic imagery and the reduced resolution outweigh the advantage of simplicity and low cost. Most systems today use temporal separation in conjunction with polarized light. The left and right image is displayed in quick succession on the same screen. In order to achieve a flicker-free display, the images must be refreshed at a rate of 60 Hz per image, requiring a 120 Hz monitor.

Two solutions are available for viewing the stereo model. As illustrated in Fig. 6.13(a), a polarization screen is mounted in front of the display unit. It polarizes the light emitted from the display in synchronization with the monitor. An operator wearing polarized glasses will only see the left image with the left eye as the polarization blocks any visual input to the right eye. During the next display cycle, the situation is reversed and the left eye is prevented from seeing the right image. The system depicted in Fig. 6.8 on page 83 employs the polarization solution.

The second solution, depicted in Fig. 6.13(b), is more popular and less expensive to realize. It is based on active eyewear containing alternating shutters, realized, for example, by *liquid crystal displays* (LCD). The synchronization with the screen is achieved

[5]Actually, only the horizontal resolution is halved while the vertical resolution remains the same as in dual monitor systems.

Figure 6.12: Example of a split-screen viewing system. Shown is the DVP digital photogrammetric workstation. Courtesy of DVP Geomatics, Inc., Quebec.

by an infrared emitter, usually mounted on top of the monitor (Fig. 6.9 on page 84 shows an example). Understandably, the goggles are heavier and more expensive compared to the simple polarizing glasses of the first solution. On the other hand, the polarizing screen and the monitor are a tightly coupled unit, offering less flexibility in the selection of monitors.

Roaming

Roaming refers to moving the 3-D pointing device. This can be accomplished in two ways. In the simpler solution, the cursor moves on the screen according to the movements of the pointing device (e.g. mouse) by the operator. The preferred solution, however, is to keep the cursor locked in the screen center, which requires redisplaying the images. This is similar to the operation of analytical plotters where the floating point mark is always in the center of the field of view.

The following discussion refers to the second solution. Suppose we have a stereo DPW with a 1280×1024 resolution, true color monitor, and imagery digitized to 15 μm pixelsize (or approximately $16K \times 16K$ pixels). Let us now freely roam within a stereomodel, much as we would do it on an analytical plotter and analyze the consequences in terms of transfer rates and memory size.

Fig. 6.14 schematically depicts the storage and graphic systems. The essential components of the graphic system include the graphics processor, the display memory,

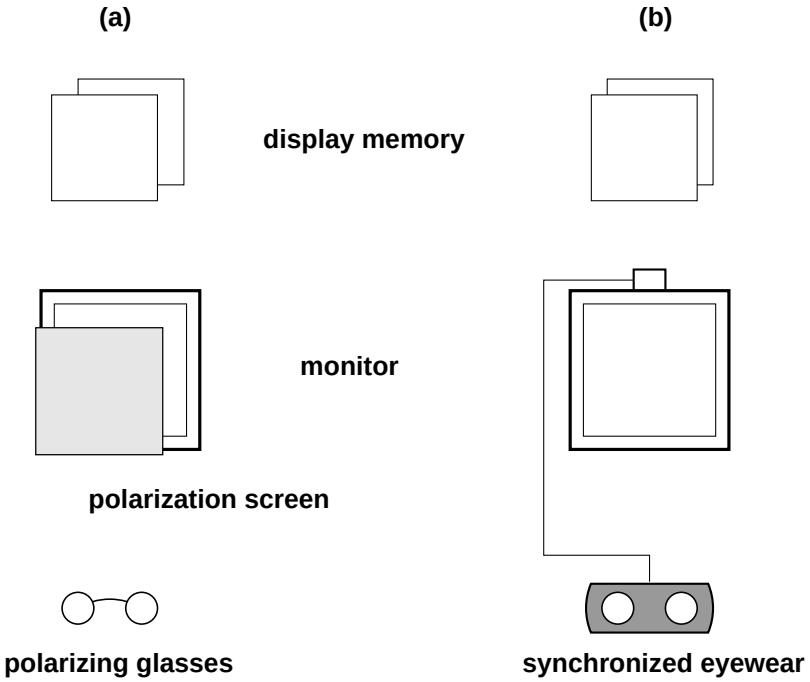

Figure 6.13: Schematic diagram of the temporal separation of the left and right image of a stereopair for stereoscopic viewing. In (a), a polarizing screen is mounted in front of the display. Another solution is sketched in (b). The screen is viewed through eyewear with alternating shutters. See text for detailed explanations.

the digital-to-analog converter (DAC), and the display device (CRT monitor in our case). The display memory contains the portion of the image that is displayed on the monitor. Usually, the display memory is larger than the screen resolution to allow roaming in real-time. As soon as we roam out of the display memory, new image data must be fetched from disk and transmitted to the graphics system.

Graphic systems come in the form of high-performance graphics boards, such as RealiZm or Vitec boards. These state-of-the-art graphics systems are as complex as the system CPU. The interaction of the graphics system with the entire DPW, e.g. requesting new image data, is a critical measure of system performance.

Factors such as storage organization, bandwidths, and additional processing cause delays in the stereo display. Let us further reflect on these issues.

With an image compression rate of three, approximately 240 MB are required to store one color image. Consequently, a 24 GB mass storage system could store 100 images on-line. By the same token, a hard disk with 2.4 GB capacity could hold 10 compressed color images.

Since we request true color display, approximately 2×4 MB are required to hold the

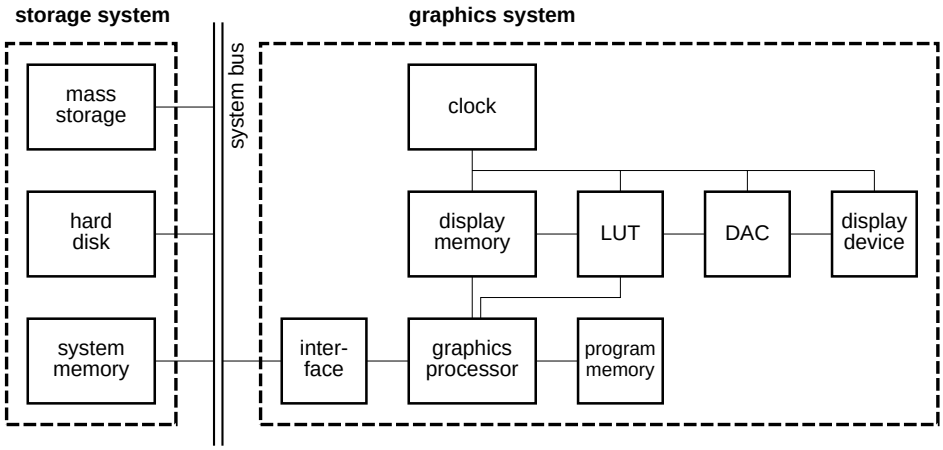

Figure 6.14: Schematic diagram of storage system, graphic system and display.

two images of the stereomodel[6]. As discussed in the previous section, the left and right image must be displayed alternately at a frequency of 120 Hz to obtain an acceptable model[7]. The bandwidth of the display memory amounts to $1280 \times 1024 \times 3 \times 120 = 472$ MB/sec. Only high speed, dual port memory, such as VRAM (video RAM) satisfies such high transfer rates. For less demanding operations, such as storing programs or fonts, less expensive memory is used in high performance graphic workstations.

At what rate should one be able to roam? Skilled operators can trace contour lines at a speed of 20 mm/sec. A reasonable request is that the display on the monitor should be "crossed" within 2 seconds, in any direction. This translates to $1280 \times 0.015/2 \approx 10$ mm/sec in our example. Some state a maximum roam rate of 200 pixels/sec on Intergraph's ImageStation Z softcopy workstation. As soon as we begin to move the pointing device, new portions of the model must be displayed. To avoid immediate disk transfer, the display memory is larger than the monitor, usually four times. Thus, we can roam without problems within a distance twice as long as the screen window at the cost of increased display memory size (32 MB of VRAM in our example).

Suppose we move the cursor with a speed of 10 mm/sec toward one edge. When will we hit the edge of the display memory? Assuming we begin at the center, after one second the edge is reached and the display memory must be updated with new data. To assure continuous roaming, at least within one stereomodel, the display memory must be updated before the screen window reaches the limit. The new position of the window is predicted by analyzing the roaming trajectory. A look-ahead algorithm determines the most likely positions and triggers the loading of image data through the hierarchy

[6] $1280 \times 1024 \times 3$ Bytes = 3,932,160 Bytes.

[7] Screen flicker is most noticeable far out in one's vision periphery. Therefore, large screen sizes require higher refresh rates. Studies indicate that for 17-inch screens refresh rates of 75 Hz are acceptable. For DPWs larger monitors are required; therefore with a refresh rate of 60 Hz for one image we still experience annoying flicker at the edges.

of the storage system.

Referring again to our example, we have one second to completely update the display memory. Given its size of 32 MB, data must be transferred at a rate of 32 MB/sec from hard disk via system bus to the display memory. The bottle necks are the interfaces, particularly the hard disk interface. Today's systems do not offer such bandwidths, except perhaps SCSI-2 devices[8]. A PCI interface (peripheral component interface) on the graphics system will easily accommodate the required bandwidth.

A possible solution around the hard disk bottleneck is to dedicate system memory for storing an even larger portion of the stereomodel, serving as sort of a relay station between hard disk and display memory. This caching technique, widely used by operating systems to increase the efficiency of data transfer disk to memory, offers additional flexibility to the roaming prediction scheme. It is quite unlikely that we will move the pointing device with a constant velocity across the entire model (features to be digitized are usually confined to rather small areas). That is, the content of the system memory does not change rapidly.

Fig. 6.15 depicts the different windows related to the size of a digital image. In our example, the size of the display window is 19.2 mm $\times$ 15.4 mm, the display memory size is $4\times$ larger, and the dedicated system memory again could be $4\times$ larger. Finally, the hard disk holds more than one stereopair.

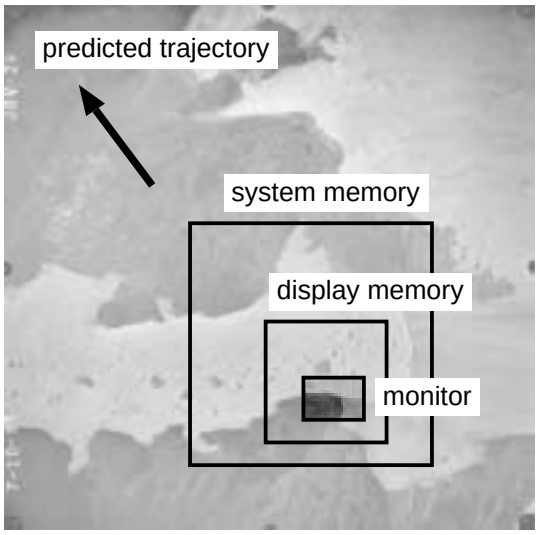

Figure 6.15: Schematic diagram of the different windows related to the size of an image. Real-time roaming is possible within the display memory. System memory holds a larger portion of the image. The location is predicted by analyzing the trajectory of recent cursor movements.

[8]Fast wide SCSI-2 devices, available as options, sustain transfer rates of 20 MB/sec. This would be sufficient for roaming within a b/w stereo model.

6.3 Analytical Plotters vs. DPWs

During the discussion of the basic system functionality and the orientation procedure, the advantages and disadvantages of DPWs became apparent. Probably the most severe shortcoming of today's DPWs is the viewing and roaming quality, which is far inferior to that of analytical plotters. Consider moving the floating point mark in an oriented model on the analytical plotter. Regardless on how quickly you move, the model is always there, viewed at superb quality. In contrast, DPWs behave poorly when an attempt is made to move the cursor from one model boundary to another.

Several factors influence the viewing quality. For one, the monitor resolution sets a limit to the size of the field of view. Small fields of view reduce the capability to stereoscopically view a model. This makes image interpretation more difficult. Flickering, particularly noticeable on large monitors, is still a nuisance, despite of 120 Hz refresh rates. A third factor is the reduction in illumination due to polarizing and alternate image displays. Finally, the ease and simplicity of optical image manipulation, such as rotation, cannot be matched on DPWs. Resampling is a time consuming process and may even reduce the image quality.

The advantages of DPWs outweigh these shortcomings by far, however. The benefits are well documented. The following are a few noteworthy factors:

- image processing capabilities are available at the operator's fingertips. Enlargements, reductions, contrast enhancements, and dodging do not require a photo lab anymore—DPWs have a built-in photo lab.
- traditional photogrammetric equipment, such as point transfer devices and comparators, are no longer required—their functionality is assumed by DPWs. Digital photogrammetric workstations are much more universal than analytical plotters.
- the absence of any moving mechanical-optical parts make DPW more reliable and potentially more accurate since no calibration procedures are necessary.
- DPWs offer more flexibility in viewing and measuring several images simultaneously. This is a great advantage in identifying and measuring control points and tie points.
- several persons can stereoscopically view a model. This is interesting for applications where design data is superimposed on a model. Free stereo viewing is also considered an advantage by many operators.
- DPW are more user friendly than analytical plotters. As more photogrammetric procedures will be automated, the operation of a DPW requires less specialized operators.

Among the many potentials of DPWs is the possibility to increase the user base. To illustrate this point, compare the skill level of an operator working on a stereoplotter, analytical plotter, and digital photogrammetry workstation. There is clearly a trend away from very special photogrammetric know-how to more generally available know-how on how to use a computer. That stereo models can be viewed without optical

mechanical devices and the possibility to embed photogrammetric processes in user friendly graphical user interfaces raises the chances that non-photogrammetrists can successfully use photogrammetric techniques.

It is possible to increase the roaming capabilities of DPWs beyond the stereomodel. Roaming should be performed in the entire project and it should include vector data, DEMs, databases, and design data. Such a generalized roaming scheme would further increase the efficiency and user friendliness of DPWs.

One of the biggest advantages, however, lies in the potential to automate photogrammetric applications, such as aerial triangulation, DEM generation, and orthophoto production.